

October 2019

Energy-Aware Algorithms for Greening Internet-Scale Distributed Systems Using Renewables

Vani Gupta

Follow this and additional works at: https://scholarworks.umass.edu/dissertations_2



Part of the [OS and Networks Commons](#)

Recommended Citation

Gupta, Vani, "Energy-Aware Algorithms for Greening Internet-Scale Distributed Systems Using Renewables" (2019). *Doctoral Dissertations*. 1741.
https://scholarworks.umass.edu/dissertations_2/1741

This Open Access Dissertation is brought to you for free and open access by the Dissertations and Theses at ScholarWorks@UMass Amherst. It has been accepted for inclusion in Doctoral Dissertations by an authorized administrator of ScholarWorks@UMass Amherst. For more information, please contact scholarworks@library.umass.edu.

**ENERGY-AWARE ALGORITHMS FOR GREENING
INTERNET-SCALE DISTRIBUTED SYSTEMS USING
RENEWABLES**

A Dissertation Presented

by

VANI GUPTA

Submitted to the Graduate School of the
University of Massachusetts Amherst in partial fulfillment
of the requirements for the degree of

DOCTOR OF PHILOSOPHY

September 2019

College of Information and Computer Sciences

© Copyright by Vani Gupta 2019

All Rights Reserved

**ENERGY-AWARE ALGORITHMS FOR GREENING
INTERNET-SCALE DISTRIBUTED SYSTEMS USING
RENEWABLES**

A Dissertation Presented

by

VANI GUPTA

Approved as to style and content by:

Prashant Shenoy, Co-chair

Ramesh Sitaraman, Co-chair

Deepak Ganesan, Member

David Irwin, Member

James Allan, Chair
College of Information and Computer Sciences

DEDICATION

To my parents, my husband, and my children.

ACKNOWLEDGMENTS

My Ph.D. studies became possible because of the contributions of several people. I have been fortunate to have Professor Prashant Shenoy and Professor Ramesh Sitaraman as my advisors. They have provided tremendous support and guidance throughout the process. Their insights into research, teaching, and academic success have helped me navigate the paths of the Ph.D. experience with greater ease. I am truly grateful for the knowledge they have shared with me. I would also like to thank Professor Deepak Ganesan and Professor David Irwin for being my committee members and for their insightful comments on my research. Their feedback has helped me analyze my research from several new perspectives.

I have had the opportunity to get to know some very talented researchers at UMass. I would like to thank Stephen Lee for being an excellent collaborator. I would also like to thank Srinivasan Iyengar for being a great resource and for his readiness to help. My sincere thanks also to all the other lab members, especially Tian Guo, Sean Barker, Ameer Trivedi and Prateek Sharma for their help.

I would like to thank Lianne Leclerc, Eileen Hamel, and Karren Sacco for taking care of the administrative details so efficiently, and for answering all my questions. I would also like to thank Valerie Caro and other CSCF members for their excellent support with technical issues and questions.

Finally, I would like to express my deepest gratitude to my family. I would like to thank my parents for their guidance, encouragement, and for all that they have done for me. A very special thank you to my two young children whose optimism and lighthearted perspective kept me going and made this journey possible. Last but certainly not the least, I am truly grateful to my husband for always being there and for supporting me every step of the way.

ABSTRACT

ENERGY-AWARE ALGORITHMS FOR GREENING INTERNET-SCALE DISTRIBUTED SYSTEMS USING RENEWABLES

SEPTEMBER 2019

VANI GUPTA

B.A., UNIVERSITY OF DELHI, DELHI

M.S., UNIVERSITY OF MISSOURI - KANSAS CITY

PH.D., UNIVERSITY OF MASSACHUSETTS AMHERST

Directed by: Professor Prashant Shenoy and Professor Ramesh Sitaraman

Internet-scale Distributed Systems (IDSs) are large distributed systems that are comprised of hundreds of thousands of servers located in hundreds of data centers around the world. A canonical example of an IDS is a content delivery network (CDN) that delivers content to users from a large global deployment of servers around the world. IDSs consume large amounts of energy and their energy requirements are projected to increase significantly in the future. With carbon emissions from data centers increasing every year, use of renewables to power data centers is critical for the sustainability of data centers and for the environment.

In this thesis we design energy-aware algorithms that leverage renewable sources of energy and study their potential to reduce brown energy consumption in IDSs. Firstly, we study the use of renewable solar energy to power IDS data centers. A net-zero IDS produces as much energy from renewables (green energy) as it needs to entirely off-set its

energy consumption. We develop effective algorithms to help minimize the number of solar panels provisioned for net-zero IDSs. We empirically evaluate our algorithms using load traces from Akamai’s global CDN and solar data from PVWatts. Our results show that for net-zero year, net-zero month, and net-zero week, our optimal algorithm can reduce the number of panels by 36%, 68%, and 82% respectively, thereby making sustainability of IDSs significantly more achievable.

IDSs consume a significant amount of energy for cooling their infrastructure. Therefore, next, we study the potential benefits of using open air cooling (OAC) to reduce the energy usage as well as the capital costs incurred by an IDS for cooling. We develop an algorithm to incorporate OAC into the IDS architecture and empirically evaluate its efficacy using extensive work load traces from Akamai’s global CDN and global weather data from NOAA. Our results show that by using OAC, a global IDS can extract a 51% cooling energy reduction during summers and a 92% reduction in the winter.

Finally, we study the greening potential of combining two contrasting sources of renewable energy, namely solar energy and open air cooling (OAC). OAC involves the use of outside air to cool data centers if the weather outside is sufficiently cold and dry. Therefore OAC is likely to be abundant in colder weather and at night-time. In contrast, solar energy generation is correlated with sunny weather and day-time. Given their contrasting natures, we study whether synthesizing these two renewable sources of energy can yield complementary benefits. Given the intermittent nature of renewable energy, we use energy storage and load shifting to facilitate the use of green energy and study trade-offs in brown energy reduction based on key parameters like battery size, number of solar panels, and radius of load movement. We do a detailed cost analysis, including amortized cost savings as well as a break-even analysis for different energy prices. Our results show that we can significantly reduce brown energy consumption by about 55% to 59% just by combining the two technologies. We can increase our savings further to between 60% to 65% by adding

load movement within a radius of 5000kms, and to between 73% to 89% by adding energy storage.

TABLE OF CONTENTS

	Page
ACKNOWLEDGMENTS	v
ABSTRACT	vi
LIST OF TABLES	xii
LIST OF FIGURES	xiv
 CHAPTER	
1. INTRODUCTION	1
1.1 Thesis Contributions	3
1.1.1 Optimal Solar Provisioning for Net-zero IDSs	4
1.1.2 Open Air Cooling (OAC) for Greening IDSs	4
1.1.3 Combining Solar Energy and OAC for Greening IDSs	4
2. BACKGROUND AND RELATED WORK	6
2.1 Background	6
2.2 Related Work	14
2.2.1 Server Level Greening	14
2.2.2 Data Center Level Greening	15
2.2.3 Network Level Greening	16
3. EFFICIENT SOLAR PROVISIONING FOR NET-ZERO INTERNET-SCALE DISTRIBUTED SYSTEMS	19
3.1 Contributions	19
3.2 Background	21
3.3 Problem and Methodology	22
3.3.1 Problem Definition	22

3.3.2	Problem Framework	23
3.4	Algorithms for Solar Provisioning in IDSs	24
3.4.1	Optimal LP Formulation	25
3.4.2	Greedy Heuristic Algorithms	32
3.4.2.1	Max Solar Per Panel Heuristic (MSP)	32
3.4.2.2	Minimum Number of Panels Heuristic (MNP)	34
3.5	Experimental Methodology	36
3.6	Empirical Results	38
3.6.1	Without Performance Constraints	38
3.6.1.1	Reduction in Number of Panels	38
3.6.1.2	Location Choices for Different Algorithms	40
3.6.1.3	Restricting Panels to Top K Data Centers	43
3.6.2	With Performance Constraints	46
3.6.2.1	Discussion on the Number of Panels	47
3.6.2.2	Location Choices for Different Algorithms	48
3.7	Implications for IDS Design	49
3.8	Related Work	50
3.9	Conclusions	51
4.	OPEN AIR COOLING FOR GREENING INTERNET-SCALE DISTRIBUTED SYSTEMS	53
4.1	Contributions	54
4.2	Background	55
4.3	A Greedy Algorithm for Exploiting OAC	57
4.4	Experimental Methodology	58
4.5	Empirical Results	61
4.5.1	Reduction in chiller capacity	61
4.5.2	Reduction in energy usage	61
4.5.3	Impact of Newer Data Center Technologies:	64
4.5.4	Network latency impact	64
4.6	Implications for IDS Design	65
4.7	Related Work	66
4.8	Conclusions	67

5. COMBINING SOLAR ENERGY AND OPEN AIR COOLING FOR GREENING INTERNET-SCALE DISTRIBUTED SYSTEMS	68
5.1 Contributions	68
5.2 Background	71
5.3 Energy-Aware Load Scheduling Algorithm	73
5.4 Experimental Methodology	75
5.5 Empirical Results	76
5.5.1 Brown Energy Reduction	77
5.5.2 Peak Reduction	82
5.5.3 Green Energy Utilization	82
5.5.4 Cost Analysis	84
5.5.4.1 Yearly Amortized Cost Savings	85
5.5.4.2 Break-even Analysis	87
5.5.5 Cost Analysis with Future Projections	88
5.5.5.1 Yearly Amortized Cost Savings with Future Cost Projections	89
5.5.5.2 Break-even Analysis with Future Cost Projections	89
5.5.6 Discussion	91
5.6 Related Work	91
5.7 Conclusions	93
6. CONCLUSIONS AND FUTURE WORK	94
6.1 Conclusions	94
6.2 Lessons Learned	95
6.3 Future Work	96
6.3.1 Exploring wind energy	96
6.3.2 Data center site selection based on renewable energy availability	97
BIBLIOGRAPHY	98

LIST OF TABLES

Table	Page
3.1 Supply Matrix	24
3.2 Demand Matrix	25
3.3 Counter example for MSP showing the algorithm is not globally optimal	33
3.4 Number of Panels Matrix	34
3.5 Parameters for PVWatts Data	36
3.6 % Panels by location for net-zero year without performance constraints	40
3.7 % Panels by location for net-zero month without performance constraints	41
3.8 % Panels by location for net-zero week without performance constraints	42
3.9 Locations under Top K Restrictions for Net-zero Year	45
3.10 Locations under Top K Restrictions for Net-zero Month	45
3.11 Locations under Top K Restrictions for Net-zero Week	46
4.1 ASHRAE’s allowable ranges for dry bulb temperature, relative humidity and the maximum dew point of the air that make it suitable for cooling different classes of data centers [35]. Higher data center classes correspond to newer technology allowing for broader ranges of tolerance.	56
4.2 Load data from Akamai CDN	59
4.3 NOAA weather data.	59
5.1 Parameters values and related notation used to refer to them in the paper	72

5.2	Parameters for PVWatts Data	75
5.3	Price and lifetime for batteries and solar panels. Cost for commercial solar panels and lithium-ion batteries was used.	84
5.4	Projected Electricity, Solar Panel and Battery Costs	89

LIST OF FIGURES

Figure	Page
2.1 Plot showing the diversity in geographic locations that can make up a global IDS	7
2.2 Solar panel facing south, with azimuth angle α and tilt angle β	9
2.3 Plot shows that there is a large variation in annual solar output depending on global location	9
2.4 Normalized monthly solar energy for Seattle showing a higher output in the summer months for the Northern hemisphere	10
2.5 Normalized monthly solar energy for Perth, Australia showing a higher output in the summer months for the Southern hemisphere	10
2.6 Normalized solar output for a week showing large daily variations in the close-by locations, and within the same location	11
3.1 Plot shows that number of panels provisioned is inversely proportional to the time period over which we aim to be net-zero	40
3.2 Plot shows that Arequipa, Peru has a high solar output consistently across all the months of the year	41
3.3 Plot shows that Arequipa, Peru has a high solar output for most weeks of the year, except a few where the plot dips	43
3.4 Number of panels provisioned are highest for net-zero week, followed by net-zero month and then net-zero year	43
3.5 Plot shows that net-zero week has the largest number of panels for any radius, then net-zero month, and finally net-zero year	48
3.6 Plot shows % decrease in number of solar panels as radius of load movement is increased. Dotted lines labeled ‘Opt_week’, ‘Opt_month’, and ‘Opt_year’ show the maximum decrease we can hope to have with an unlimited radius.	49

3.7	Plot shows that the number of locations where panels are allocated decrease as we increase the radius of load movement. This is because the load converges to global locations with high solar output	50
3.8	Distribution of panels for 500kms for different net-zero time periods showing that the number of locations is largest for net-zero week, then for net-zero month, and finally for net-zero year	51
3.9	Locations where the LP with performance constraints send the load to for net-zero month	51
4.1	Normalized cooling energy required by Akamai's CDN in the US, UK, Japan and Australia. Notice the diurnal variation as cooling energy is proportional to the load induced by users accessing content from those locations.	60
4.2	Savings in capital costs of chillers with OAC.	62
4.3	Energy savings for the entire global IDS and for major countries in each of the two hemispheres.	62
4.4	Regional and seasonal variations in OAC savings in Japan and Singapore.	63
4.5	Energy savings for the entire global IDS and for major countries in each of the two hemispheres for A2 data centers.	65
4.6	Average distance the load is moved by our algorithm for the whole year and on the worst day for $r = 500$ and 1000	65
5.1	Plot shows how solar energy and OAC combine to yield higher savings across various months of the year for panels0.5 and $r=0$	77
5.2	Figures show the break-up of brown energy reduction for only solar, only oac, and solar plus oac with bcap0 and panels0.5nzy	78
5.3	Figures show the break-up of brown energy reduction for only solar, only oac, and solar plus oac with net metering and panels0.5nzy	79
5.4	We see a significant increase in brown energy reduction as we move from solar energy only (a & c) to solar energy + OAC (b & d). Increasing r (a & b) yields larger savings. Increasing battery capacity (c & d) helps but shows diminishing returns.	80

5.5	Figure showing reduction in brown energy across different months for Anchorage and Las Vegas	81
5.6	Plot showing significant gains in peak reduction. Increasing solar panels, battery capacity and r result in higher reductions.	82
5.7	Plots show that batteries help with increasing green energy utilization. Load movement also helps in increasing green energy utilization over larger values of r	84
5.8	Plots show significant amortized savings for moderate and high energy prices. For the lower energy price, we see losses for higher battery capacity and larger number of panels. However, even for the lower energy price, we see significant savings without batteries, and we can see some savings with bcap0.5.	85
5.9	Plot shows a decrease in the number of years to break even as the price of energy goes up (for r=0).	87
5.10	The break even period is inversely proportional to the price of energy. With a moderate amount of battery capacity and panels, we can achieve close to the lowest break even periods compared to others.	88
5.11	Future projection plots show dramatic increases in amortized savings for moderate and high energy prices. For the lower energy price scenario for r=0, we see a savings of 23.9% to 55.9% with no losses for any combination. This is an improvement from the current price scenario.	90
5.12	Plot shows a significant decrease in the number of years to break-even with future cost projections (for r=0).	90

CHAPTER 1

INTRODUCTION

Modern Internet services are delivered by Internet-scale distributed systems (IDSs) that consist of hundreds of thousands of servers deployed in a large number of data centers around the world. IDSs include cloud and Internet services such as content delivery networks (CDNs) that deliver web content, applications, and streaming media to clients on the web via hundreds of thousands of servers located in thousands of data center locations throughout the world [53]. An IDS consumes a significant amount of energy to power its servers and to cool them. It is not uncommon for a large IDS to incur energy bills that run into millions of dollars per month. The environmental impact of data center energy consumption is also concerning. U.S. data centers are projected to consume approximately 73 billion kWh in 2020 [61]. Thus, it is imperative to re-design IDSs with energy as a key design consideration to ensure the sustainable growth of these networks.

Given the tremendous energy requirements of IDSs, data centers that are powered using renewables are gaining a lot of traction the industry and the research community. In just six years, Apple's use of renewable energy to power its corporate facilities, retail stores, and data centers worldwide went from 16 percent in 2010 to 96 percent in 2016 [1]. Apple is now committed to powering all their facilities world-wide with 100% renewable energy. In 2017, Google achieved the milestone of purchasing 100% renewable energy to match consumption for global operations, including their data centers and offices [4].

There has been a lot of work done in the research community on making data centers greener by reducing energy consumption or using energy generated from renewable sources. Prior work includes energy reduction using server shutdown or low-power states during off-

peak times [44] [49] [17] [60]. There is also work on job scheduling based on predicted solar [29] [28] and load balancing to encourage use of renewable energy [47] [46] [27]. Separately there has been work on selecting sites for and provisioning green data centers using a follow-the-renewables approach [13]. Greening IDSs is now a necessity for sustainable growth of IDSs, for reducing environmental impact, and for lowering energy costs for companies. Major IT companies, like Google and Apple, use a combination of methods to green their operations. Google is trying to achieve 100% clean renewables by generating some green energy on-site, but mainly by acquiring Renewable Energy Credits (RECs) through their Power Purchase Agreements (PPAs) with renewable energy companies [4]. PPAs are contracts that allow companies to buy power from energy companies at negotiated prices. RECs are a means to keep track of who is using and consuming green energy. Companies create a REC if they generate a MWh of green energy and consume a REC if they consume a MWh of green energy. Google enters into PPAs with renewable energy companies and buys renewable energy from them. Thereafter Google sells the energy back on the grid. This indirect way of generating green energy gets Google RECs that they then use to offset their grid energy use. Apple produces its own green energy where possible, and then it also relies on PPAs and RECs to fully green its operations [1].

Renewables sources of energy like solar energy, wind energy, open air cooling have great potential to meet our energy needs, but they are only available at certain times, to different degrees, and in certain locations around the globe. IDSs such as CDNs have two defining characteristics: *a global deployment* of servers in multiple data centers around the world, and *a replication* of services across these data centers. The global deployment is often driven by the need for an IDS to have servers “proximal” to the end-users. A corollary of this deployment model is that it is not possible for IDSs to deploy *only* in places where renewables are available for most of the year. They need to be deployed near where the users are. However, IDSs often replicate their services across their data centers, so that the workload of serving users can be easily shifted from one data center to another, albeit

with a potential for performance degradation. These two characteristics provide an IDS the flexibility to move its workload across data centers to exploit climatic variations to optimize the use of renewables, a flexibility that services employing a single or a few data centers do not possess. It is in this sense that, even though IDSs consume massive amounts of energy, they lend themselves well to greening. We take advantage of this factor extensively in our thesis to help us achieve our goal of greening IDSs.

Solar energy is one of the cleanest and most abundant source of renewable energy available [65]. Large IT companies such as Apple and Google are committing to solar to meet some of their data center energy needs. Apple has recently announced that it plans to build a 200MW photovoltaic solar capacity in a joint venture with Nevada Energy (NV Energy) to power its data center in Reno, Nevada [10]. Google is set to power its recently opened Dutch data center containing thousands of servers with solar energy [32]. We also know that for data centers in general, cooling is a significant source of energy consumption. In addition, the American Society of Heating, Refrigerating and Air-Conditioning Engineers (ASHRAE) relaxed the limits on operating temperatures and humidity ranges for data centers, and defined new classes of data centers that can tolerate higher temperatures and humidity levels [35]. These facts coupled with the ability to address both server and cooling energy make solar and OAC attractive technologies to focus on. Our motivation for using solar and OAC stems from the fact that by addressing both the cost of powering and cooling servers we can offer a more comprehensive energy reduction solution for IDSs. In addition, motivated by the contrasting natures of the two technologies, we study if there are any complementary benefits in combining them for greening IDSs.

1.1 Thesis Contributions

This thesis proposes novel techniques to incorporate the use of renewables in global IDSs with an aim to reduce capital and operational costs, as well as to green IDSs. We design

energy-aware algorithms that leverage renewable sources of energy and study their potential to reduce brown energy consumption in IDSs. We outline three specific contributions below.

1.1.1 Optimal Solar Provisioning for Net-zero IDSs

A net-zero IDS produces enough green energy to off-set its brown energy consumption. We study the potential of solar energy for powering global net-zero IDSs. We develop novel greedy and optimal algorithms to enable load shifting for different net-zero time periods. We study the impact of unrestricted load movement, restricting solar panel provisioning to certain locations, and restricting load movement within different radii, on the reduction in the number of solar panels. We extensively evaluate our work using Akamai CDN’s load traces, and solar data from PVWatts. Overall, with unrestricted load movement, we can reduce the number of solar panels by 36%, 68%, and 82% for net-zero year, net-zero month and net-zero week respectively.

1.1.2 Open Air Cooling (OAC) for Greening IDSs

We study the potential of OAC to reduce energy consumption in IDSs. We develop a simple greedy algorithm that allows us to move load to leverage OAC. We design the algorithm to enable us to enforce performance constraints by restricting the radius of load movement. We evaluate our work using extensive load traces from Akamai’s CDN and NOAA weather data. We demonstrate the benefits of OAC by showing we can reduce cooling energy by 51% in the hot months of summer, and by 92% in winter, when the temperatures are lower.

1.1.3 Combining Solar Energy and OAC for Greening IDSs

Finally, we study the use of OAC and solar energy in conjunction with each other to green IDSs. Solar energy is associated with day-time and sunny weather. OAC is associated with night-time and colder weather. In this work, we design a simple greedy heuristic algorithm and study the greening potential of combining solar energy and OAC with respect

to energy savings, energy utilization, and cost savings. Both these sources of renewable energy are intermittent, so we use energy storage and load shifting to facilitate the use of green energy and study trade-offs in brown energy reduction based on key parameters like battery size, number of solar panels, and radius of load movement. We do a detailed cost analysis, including amortized cost savings as well as a break-even analysis for different energy prices. Our results look encouraging and we find that we can significantly reduce brown energy consumption by about 55% to 59% just by combining the two technologies. We can increase our savings further to between 60% to 65% by adding load movement within a radius of 5000kms, and to between 73% to 89% by adding energy storage.

CHAPTER 2

BACKGROUND AND RELATED WORK

This chapter provides a background on Internet-scale Distributed Systems (IDSs). We also discuss related work on the use of renewables in data centers.

2.1 Background

Internet-scale Distributed Systems: Internet-scale Distributed Systems (IDSs) are large-scale global networks that are comprised of data centers in several locations across the world. Content delivery networks (CDNs) are examples of IDSs and are used to deliver content, streaming audio, video, applications etc. on the web. Figure 2.1 shows data center locations part of the Akamai CDN. Commercial CDNs use two levels of load-balancing in their systems: *local* and *global*. When a user requests content, the *global* load-balancer assigns the request to a server cluster located ‘close-by’ to minimize loss and latency [53]. The *local* load-balancer then maps the request to a specific server in the cluster. In order to assign users to nearby data centers and minimize loss and latency, CDNs replicate their services so as to have redundancy in the choice of data centers. This replication is also very useful if load from one data center is assigned to another data center for any other reason, e.g. to leverage a local feature like high solar output.

Energy for Powering Servers: The primary source of energy consumption in IDSs are the numerous servers deployed in all the various data centers (*server energy*). The energy consumed by a server is largely dependent on the amount of load it is serving, so we can model the energy consumed by a server as a function of its load. However, servers are not energy proportional and still consume some energy, roughly 60%, when they are idle. The

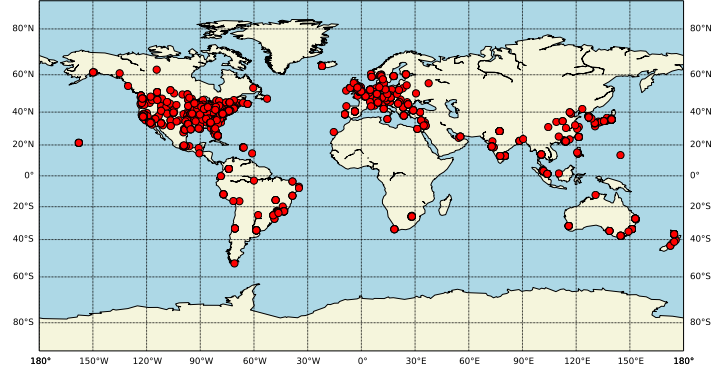


Figure 2.1: Plot showing the diversity in geographic locations that can make up a global IDS

standard linear model of server power consumption [12] that defines power consumed by a server as $P_{idle} + (P_{peak} - P_{idle})\lambda$, where λ is the normalized load on the server, P_{idle} is the power consumed by server that is idle, and P_{peak} is the power consumed by the server that has peak load. We assume that we can move load between servers to consolidate load, and shut down idle servers, so as to use the minimum number of servers needed to serve the load [43]. In order to determine the power used by a cluster of servers in a data center, we first use the total load for the data center l and the capacity c of each server to find out how many servers we need to consolidate our load as $w + f = l/c$, where w is the number of whole servers, and f is the fraction of a last server needed. We then calculate the consolidated power as $P_{peak} * w + P_{idle} + (P_{peak} - P_{idle}) * f$. Power consumed (in Watts) by the cluster in each 5-minute time interval is then multiplied by the number of seconds ($5*60$) to get the energy consumed by the cluster in each time interval (in Joules). Our assumption is that such consolidation of load is done at each of the data center locations for each time period.

Energy for Cooling Servers: In addition to the energy needed to run servers, we also need energy to cool them (*cooling energy*). Heat dissipated by servers is a function of the energy they consume. The more heat they dissipate, the more energy is needed to cool them down. So cooling energy is proportional to server energy. The proportionality factor models

how efficient the cooling system is and reflected by the power usage effectiveness (PUE) of a facility. Power usage effectiveness (PUE) is defined as the ratio of the total energy consumed by the facility, to the energy delivered to computing equipment. Though efficient data centers with lower PUE exist, the average PUE of a data center is shown to be 1.8 [69]. Therefore cooling energy accounts for a large fraction of the total energy requirements of an IDS.

Solar Arrays and Factors Affecting Solar Output: A solar panel is an electrical device that converts sunlight into electricity using the photovoltaic effect. A solar array consists of several solar panels that can be configured for efficiently generating solar energy. There are several factors that affect solar output from solar arrays, but they can be essentially divided into two categories: factors affecting how efficiently the panel is able to utilize the solar radiation it receives (*configurable*) and factors affecting the amount of solar radiation reaching the panel (*non-configurable*):

Configurable factors are those that can be changed to see a change in the output. These are related to the type of panels installed, their tilt, objects that shade the panel etc. Some of these are listed below:

- *Module Type and Array Type:* A solar module or solar panel can be standard, premium or thin film. Standard includes typical poly- or mono-crystalline silicon modules, with efficiencies in the range of 14-17%. Premium modules have a higher efficiency and thin film modules have a lower efficiency than the standard module [20]. For our experiments, we have chosen the ‘Standard’ module. Arrays also come in different varieties and can be either mounted in a fixed manner, or rack mounted to track the sun. Sun tracking arrays yield more solar output, but are harder to maintain because of the tracking rack and are more expensive [3]. For simplification, we have used a ‘Fixed Open Rack’ configuration for our experiments.
- *Tilt and Azimuth Angle:* The tilt angle, β , is the angle at which the solar panel is inclined to the horizontal and is shown in Figure 2.2. There are several sophisticated

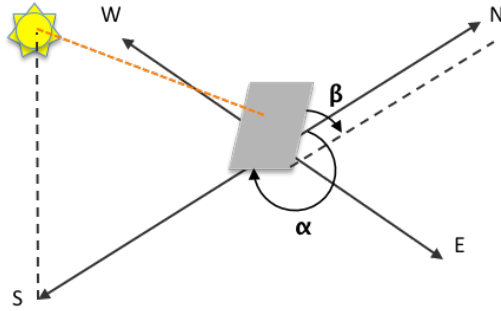


Figure 2.2: Solar panel facing south, with azimuth angle α and tilt angle β

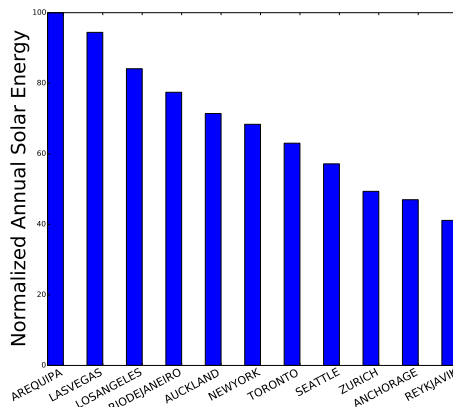


Figure 2.3: Plot shows that there is a large variation in annual solar output depending on global location

ways to calculate optimal tilt, however, as a general rule a fixed tilt angle equal to the site's latitude is often recommended [6]. The azimuth angle, α , is defined as the angle clockwise from true north of the direction that the PV array faces, and is shown in Figure 2.2. Therefore, the azimuth angle for locations in the northern hemisphere is 180 degrees, and for locations in the southern hemisphere it is 0 degree.

Non-configurable factors that cannot be changed to increase output and are outside the control of panel owners. These are mainly a function of the location, geography, like weather, seasons etc. We discuss some of these factors below:

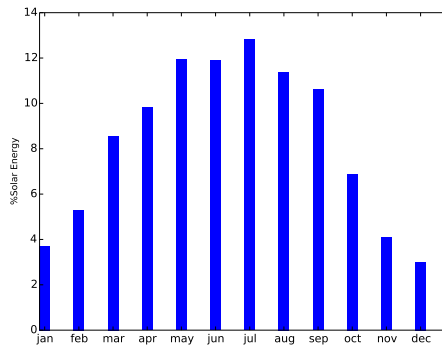


Figure 2.4: Normalized monthly solar energy for Seattle showing a higher output in the summer months for the Northern hemisphere

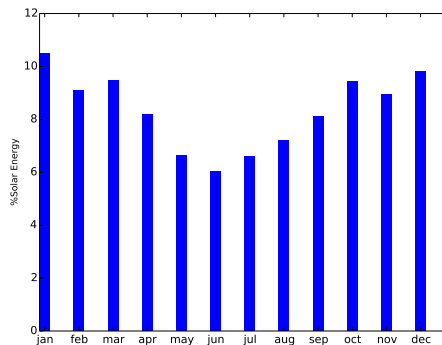


Figure 2.5: Normalized monthly solar energy for Perth, Australia showing a higher output in the summer months for the Southern hemisphere

- *Temperature:* Solar panels are tested at 25 °C , and come with a temperature coefficient value that is expressed as a percentage per degree Celsius (e.g. -0.5% per °C). At higher temperatures, beyond 25 °C , solar panel efficiency declines by the amount of its temperature coefficient percent for every 1 °C rise in temperature [2].
- *Location:* As shown in Figure 2.3, there is a large variation in annual solar output based on location. The total solar irradiance is the maximum amount of irradiance that can be received and is possible when the sun’s rays strike the earth at 90 degree angle. As you move further away from the equator, the rays are less perpendicular

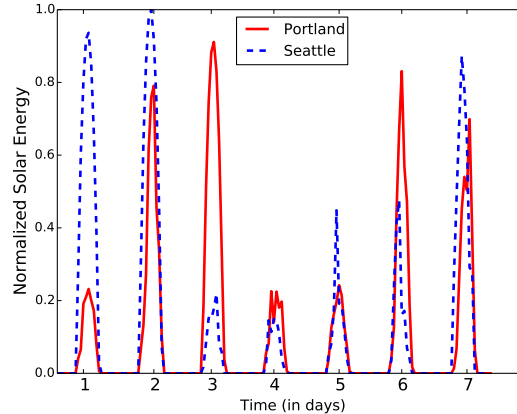


Figure 2.6: Normalized solar output for a week showing large daily variations in the close-by locations, and within the same location

and therefore cover a larger area. Therefore, the solar irradiance received per unit area is not as concentrated. The latitude of a location determines whether it is close to the equator or farther away, which in turn determines how direct the incoming solar radiation is. This factor leads to a decrease in the amount of solar irradiance as we move to higher and higher latitudes.

- *Season:* Solar output also varies by season. Summer months tend to have higher levels of solar than winter months. This can be seen in Figure 2.4 which shows the monthly solar output for Seattle, WA.
- *Hemisphere:* Winter months in the northern hemisphere are summer months in the southern hemisphere and vice versa. This factor affects the amount of solar output for panels placed in different hemispheres. Figures 2.4 and 2.5 show monthly solar output for Seattle in the northern hemisphere and for Perth in the southern hemisphere. As we see, the trend in the levels of solar output is reversed for these locations, given winter in the northern hemisphere is summer for the southern hemisphere, and vice versa.

- *Daily variations:* Solar output goes to zero when the sun is not shining and so the hour of the day affects solar output. As Figure 2.6 shows, for each location there are hours when solar is zero and then it rises steadily, peaks and then falls again once the sun sets.
- *Other factors:* All other factors like location, season, and time of day remaining constant, solar output can still change based on several factors that may include weather, cloud cover, pollution etc. As Figure 2.6 shows, within the same location, season, hemisphere and time of day, we see large variations between solar output from one day of the week to the next. Locations that are close-by e.g. Portland, OR and Seattle, WA also show large variations in solar output, as we can see in the figure.

Given the above analysis, we conclude that solar output is highly variable across time and space and is affected by several diverse factors, and their interplay. While this is a challenge as it leads to intermittent solar power availability, it is also an opportunity in the context of a global IDS that can leverage high levels of solar by moving load to those locations. In our study, we leverage these complex variations to reduce the number of panels provisioned.

Open Air Cooling (OAC): Data centers need to keep their IT equipment at prescribed temperatures to keep them from failing. Chillers are typically used by data center to cool servers by drawing hot air from the servers through a series of coils containing chilled water. This leads to an increase in the temperature of the water, which is then taken to a cooling tower to be cooled [19]. Chillers consume immense amounts of energy and must be kept on constantly to maintain the right temperature levels. A promising approach for reducing the cooling energy of a data center is to use the outside air, instead of chillers, to cool servers within the data center - these techniques are broadly referred to as Open Air Cooling (OAC). OAC works by drawing into the data center cool outside air, if required mixing it with warmer indoor air to maintain appropriate temperature and humidity levels, and to supply

that air to the cold aisles in the data center [54]. The intake air may also be filtered to limit contamination. This approach has the potential to reduce or even fully eliminate the need for chillers that consume much of the electrical energy used for cooling. Different forms of OAC include evaporative cooling, which uses a combination of water and outside air, and direct air cooling, which directly uses outside air, to cool servers. Our analysis is agnostic to the exact form of OAC employed by the data center.

OAC has recently been successfully installed in a few facilities such as Facebook's data center in Forest City, North Carolina [68]. However, OAC is feasible only when the air is "cold" and "dry" enough. As a result, OAC may not be possible everywhere. Further, even where OAC is possible, it may not be possible during all times of the day, or all seasons of the year.

Net-zero Systems: A net-zero energy data center is designed and managed in a manner that uses on-site renewables to entirely offset the use of any non-renewable energy from the grid [11]. Extending this basic definition for the purposes of this paper, we define a net-zero' IDS for different time periods as below:

- *Net-zero Year IDS:* A net-zero year IDS is one that consumes as much energy in a year as it produces in a year using renewables.
- *Net-zero Month IDS:* A net-zero month IDS is one that consumes as much energy in a month as it produces in a month using renewables, for every month in a year.
- *Net-zero Week IDS:* A net-zero year IDS is one that consumes as much energy in a week as it produces in a week using renewables, for every week in a year.

Based on the above definitions, net-zero week is the most stringent requirement. For and IDS to be net-zero week, it must be net-zero during every week of the year, including the worst week in terms of solar energy output as well. If an IDS is net-zero week, clearly, it is also net-zero month and net-zero year. Similarly, if an IDS is net-zero month, it is also net-zero year.

2.2 Related Work

Due to the tremendous energy needs of data centers, use of renewables (e.g. wind energy, solar energy etc.) has become critical to the sustainability of data centers and for the environment. Therefore, solutions for greening data centers are fast gaining momentum in research and in the industry. Prior work in the area of renewables can be categorized by scale as follows: server level, data center level, and network level. Mostly, server level studies focus on reducing energy consumption of individual servers by various methods of power management. Data center level work mainly focuses on capacity planning of data center, workload management for a data center, and reducing cooling costs for individual data centers. Network level studies focus on geographical load balancing and siting and provisioning data centers and renewables. We discuss these studies in the sections below.

2.2.1 Server Level Greening

Prior work includes studies to manage server power states in order to save energy. SolarCore [42] is a power management solution for solar powered multi-processors. SolarCore use heuristics to allocate solar power between cores, so as to increase the utilization of solar energy. Motivated by the need to use renewable energy in data centers that is characterized by intermittency, Blink [60] enables systems to handle interruptions in power supply by using transitions between high powered active states and low powered inactive states. There has also been other studies aimed at reducing energy consumption in data centers, including solutions focused on shutting down servers or clusters during off-peak periods and/or using low-power consumption states instead of powering them off in order to prevent wear and tear [44] [49] [17]. Studies have also been done on power management at the operating system level. Studies have also been done at the OS level to efficiently manage power consumption without degrading performance. On-demand governor [55] is a real-time power manager for Linux that monitors the CPU several times and sets clock frequency and supply voltage according to load and with the aim of keeping the CPU 80% utilized.

ECOsystem [72] allocates energy between applications on battery powered devices based on users' application priorities and target battery lifetime. These studies provide excellent solutions for server energy management and savings, however, they do not deal directly with renewable energy utilization/provisioning at the intra-data center IDS level.

2.2.2 Data Center Level Greening

Solutions that leverage renewables have also considered intra-data center workload scheduling. Parasol is a prototype powered by renewables [28] and was developed to study the use of solar energy for a data center. GreenSlot [29] and GreenHadoop [30] are two job-scheduling systems that schedule jobs in a way that maximizes the use of solar energy, without violating job deadlines. If energy from the grid is to be used, the scheduler tries to schedule the job when the price of energy is cheap. An adaptive scheduler for mixed batch and web service jobs has also been developed [9] that utilizes solar and wind energy prediction to decrease canceled jobs and increase green energy usage efficiency. An agile computing cluster [39] has also been developed that defers batch jobs and gracefully degrades interactive services and utilizes wind energy. iSwitch [41] matches variable load to intermittent power supply by dividing servers into two groups (one containing servers powered by the grid and the other powered by wind energy) and migrating jobs to maximize wind energy use.

Under capacity planning, ReRack [15] is a simulator that calculates the energy cost of a data center using renewable energy. For a given location and workload, ReRack finds the best ratio of renewables. Work has also been done in optimization-based energy capacity planning with the aim of meeting carbon footprint goals, by incorporating not only on-site renewables, but also using off-site renewables, power purchase agreements (PPAs), and renewable energy credits (RECs) [58].

It takes almost as much energy to cool a data center as it takes to power it. Therefore, some studies have also looked into harnessing renewable open air cooling to reduce cooling

costs in data centers. Prior work has looked into various cooling technologies, including open air cooling, in the context of modular data centers [38]. Their focus is on evaluating different cooling technologies in various climates for modular data centers, rather than on load shifting to leverage climatic conditions to increase open air cooling. Separately, work has been done in the area of unified management of data centers depending upon intermittency of renewables, cooling efficiency, differences in workload levels and energy price fluctuations [16]. This work however is distinct from ours as it focuses on workload management for individual data centers and does not leverage inter-data center load movement for renewable energy optimization.

2.2.3 Network Level Greening

All the above studies provide solutions for solving a range of problems associated with greening data centers, however, they are all at the individual data center level, with no load movement between data centers. Separately, work has been done in the area of inter-data center load balancing. FreeLunch [8] proposes a network of inter-connected data centers in which migration of virtual machines is done based on the availability of renewable energy, including solar and wind. This study presents a more high-level motivation and outline and does not present formal algorithms or an evaluation using real world traces and weather data. A trace-driven evaluation has also been done to move load between data centers using a ‘follow the renewables’ approach [47]. Additionally, [46] study investigates the use of renewables (wind and solar) to almost entirely power data centers. However, both their solutions using renewables like solar are for *load-balancing* and not optimal *solar provisioning* over different time periods. Also, they model a smaller network of data centers, much smaller in scale than the Akamai network whose trace we use to evaluate our work. In addition, they do not consider open air cooling as part of their renewable mix. Differently, there are studies that look into user request routing for greening data centers. In this study [66], request-level energy profiling is used to route requests to data centers where renewables

are available. Another study [73], proposes a middleware solution for dispatching requests to data centers, based on weather conditions conducive to maximizing renewable energy use and at the same time staying within an operational budget. Once again, our work is distinct in that we move load in an off-line fashion to determine renewable use potential and provisioning, rather than for online load balancing. Also, we use load, rather than requests, as a means to determine energy requirements for a data center. FORTE [27] assigns users and data objects to data centers based on the optimization of latency, price of electricity, and carbon footprint. Their method is online request routing which is different than our offline provisioning to optimize renewable potential. In addition, they do not explicitly consider open air cooling as part of their renewable mix.

Previous work has also looked into providing a solution for selecting sites for and provisioning green data centers using a follow-the-renewables approach [13]. However, their work focuses on siting and provisioning data centers and associated green power plants from scratch based on the availability of wind and solar and various other costs, where as our data center locations are given. In addition, they base the placement of their data centers partially on a combination of availability of solar and wind energy. In contrast, our decisions are driven by the availability of solar and open air cooling. The problem framework and solutions are different as they do not consider the impact of achieving net-zero status over different time periods. In addition, they do not study the impact on panel provisioning of moving load within radii of different distances around each data center.

In this thesis, we focus our attention on two renewable sources of energy: solar energy and open air cooling (OAC). We first study the optimal provisioning of solar panels for net-zero IDSs. In the next part of the thesis, we study the benefits of using renewable free OAC to cool IDSs. We finally study the two technologies in conjunction with each other to further optimize the use of green energy in IDSs. To the best of our knowledge, prior scientific studies have not examined the potential benefits of exploiting OAC at a global scale by a distributed network deployed across a large number of data centers, that is part

of the focus of our work. In addition, to the best of our knowledge, prior work has not addressed optimal solar panel provisioning for an existing net-zero IDS at a global scale.

We use four levers to allow us to green IDSs and to harness intermittent renewable energy in geographically distributed locations of the IDS. These levers are renewable power, renewable cooling, load shifting to use remote renewable power and cooling, and energy storage. Renewable energy output varies both by space and time. To take advantage of renewable output variations in space, we use load shifting constrained by different radii of load movement. To utilize time based variations, we use net-metering and energy storage. Net-metering allows us to put excess instantaneous renewable generation back onto the grid. Both net-metering and storage enable us to smooth the supply of renewable energy in time and prevent extra instantaneous renewable energy from being wasted. Each of these levers has an associated cost and benefit. There is a capital expenditure for installing solar panels and for setting up the infrastructure needed to enable OAC. Similarly there is a latency cost of moving load and a capital expense for installing energy storage. On the flip side, there are benefits of using these four levers. Renewable solar and cooling enable us to replace brown energy with green energy. Load shifting allows us to better utilize remote renewable power and cooling. Energy storage enables us to better utilize local renewable energy at a later time. In addition, these levers can be substituted for each other in varying degrees for reducing brown energy consumption. E.g. by installing a greater number of panels and a higher capacity energy storage system, we might be able to avoid load shifting thereby not incurring latency - although at a higher cost for the extra panels and energy storage. These types of trade-offs and substitutability between the four levers considered are interesting from a research standpoint and we try to quantify them for our data set.

CHAPTER 3

EFFICIENT SOLAR PROVISIONING FOR NET-ZERO INTERNET-SCALE DISTRIBUTED SYSTEMS

In this chapter, we focus our attention on the optimal provisioning of solar panels to green IDSs. When a system produces enough green energy to off-set its energy use over a time period, it is said to be ‘*net-zero*’ over that time period. E.g. if a system produces enough green energy to off-set its energy use over a month, we say that it is a ‘*net-zero month*’ system. The energy IDSs consume is dependent on factors like the load they serve, the number of servers that are active at any given point in time, and the energy required to cool servers. We refer to this energy as the *energy demand*. On the other hand, the solar output of the panels is the *energy supply*. In order to be net-zero over a time period, our problem is to match the *energy demand* with the *energy supply* in that time period. Often in the industry net-zero energy buildings are defined to be net-zero on an annual basis [36]. In this part of the thesis, we study the solar potential of being net-zero over different time periods including a week, a month and a year, while also ensuring that we provision the minimum number of panels to meet the demand.

3.1 Contributions

- *Determining Solar Potential for Global IDSs:* To the best of our knowledge, this is the first study to look into the net-zero solar potential for existing global IDSs comprising of data centers located in hundreds of locations throughout the world. In order to reduce the number of panels provisioned, we leverage global locations that have high solar output for different time periods. By moving load to locations

with high solar output, we can meet the system demand with fewer number of panels as each panel yields higher output. To determine the number of panels needed for achieving a net-zero system, we move load in an off-line fashion and ensure that the data center energy demand is matched by solar energy supply for each time period.

- *Algorithm Design:* We design an optimal LP algorithm to minimize the number of panels we need to server the load, by taking advantage of higher level of solar across various regions on the globe. If we allow an unrestricted radius of load movement, the time complexity of this LP becomes high. So for those cases, we reformulate the LP with a reduced set of variables and constraints, ensuring it is equivalent to the earlier formulation. To further reduce time complexity, we also propose greedy heuristic algorithms and study their effectiveness in reducing the number of panels when compared to the optimal LP. We design our algorithms such that they can be generalized to different net-zero time periods, including net-zero week, month, and year. We also design the LP to study the impact of restricting load movement within a certain radius when determining the number of panels to be provisioned.
- *Extensive Trace-based Evaluation:* We evaluate our algorithms for net-zero week, month and year on an extensive load trace from one of the world's largest CDN. The trace consists of five-minute information from 100,592 servers in over 724 global data center locations for Akamai's CDN. We see significant reduction in the number of panels and also find that our heuristic algorithms perform well compared to the optimal LP. Overall, if we allow unrestricted radius of load movement, we find that we are able to reduce the number of solar panels by 36% for net-zero year. For net-zero month by about 67% to 68%, and for net-zero week between 71% and 74% for the heuristics. The LP yields a much higher reduction of 82% for the net-zero week case. Our solution provisions panels by taking advantage of global locations with high solar output. We study the impact of restricting the radius of load movement on the

reduction in the number of panels. We see that we can gain significant reductions even when we are constrained within small radii. E.g. for net-zero month, with a radius of 500kms, we see over a 27% reduction in the number of panels. For net-zero week, the reduction is even more significant, with a radius of 200kms yielding a reduction of 31% in the number of panels.

3.2 Background

Solar Energy: Solar energy is energy harnessed from the sun and is the cleanest and most abundant form of renewable energy available [65]. A solar panel is an electrical device that converts sunlight into electricity using the photovoltaic effect. Solar arrays consist of many solar panels and when sunlight hits these arrays, they produce electricity. As detailed in Chapter 2, solar generation is intermittent and is impacted by several factors such as seasons, weather, time of day, and location.

Methods of Utilizing Renewables: There are multiple ways in which a data center can utilize green energy for its operations. One way is for data centers that install solar arrays on-site and directly draw from them to power their operations. However, due to the fact that solar energy is an intermittent source, these data centers cannot always rely on the availability of solar. One way to get around the intermittency of solar is to use batteries that allow excess instantaneous solar energy to be stored for use at a later time when solar energy might not be available. Another way is to draw energy from the grid as and when there is demand, and put back excess instantaneous solar energy onto the grid when there is excess production. This is called net metering [5]. So IDs can provision solar panels in all or some of their data center locations to match their brown energy consumption. Given that solar output is heavily dependent on the location, where such panels are provisioned significantly impacts the number of panels that will be needed to offset their energy consumption. Whichever method of incorporating solar is used (direct on-site use, batteries or net metering), companies can benefit from installing a minimum number of panels at locations where solar output is high.

Determining how solar panel provisioning can be optimized for different net-zero time periods for IDSs is the main topic of this paper. We use net-zero year to mean a system that generates as much energy from solar as it draws from the grid over a year. We similarly use net-zero month, and net-zero week to mean systems that are net-zero over a month, and week respectively. Our algorithms study the impact of being net-zero for each of these time periods.

3.3 Problem and Methodology

Data centers consume energy to maintain, run, and cool servers and other equipment. For a net-zero data center, energy supply needs to be matched by the demand using energy generated from renewables, like solar. There is a large variation in solar output across global locations, with certain locations being excellent for solar generation. In this paper, we address the problem of optimal provisioning of solar panels at data center locations with high solar to match energy demand and reach net-zero status over various time periods.

While defining the problem, we make two simplifying assumptions. It is possible to install as many solar panels as we need in any location. Secondly, it is possible to deploy as many servers as we need at any location.

3.3.1 Problem Definition

At a high level, we define the solar provisioning problem we address in this paper as below:

Solar Provisioning Problem: Our goal is to minimize the number of solar panels provisioned to achieve net-zero status by moving load to locations with higher solar output.

More specifically, we study the following research questions:

- *How can we be net-zero over different time periods:* We study the impact on the number of panels for achieving net-zero status over different time periods, including net-zero week, net-zero month, and net-zero year.

- *How can we be net-zero without performance constraints:* In order to provision panels, we assign load in a way that takes advantage of high levels of solar in various locations. To determine our full solar potential, we analyze how much reduction we can see in the number of panels if we allow load to be assigned to any location on the globe, without worrying about performance or latency. This scenario obviously yields best case results for reduction in the number of panels, and becomes a point of comparison for results under more constrained scenarios. We do this analysis for each of the above time periods.
- *How can we be net-zero without performance constraints, with panels assigned to top k locations only:* For an IDS data centers sizes vary by location and population. Generally speaking, areas with larger population tend to have larger data centers so servers can be proximal to users in order to reduce latency and loss. We use the number of servers as an indicator for the size of the data center. In this scenario, we sort our data centers by the number of servers they have and consider only the top k locations as candidates for installing panels. We study how the number of panels provisioned change as we vary k.
- *How can we be net-zero with performance constraints:* In order to keep latency down, keeping load closer to its original location is important. This scenario allows us to put constraints on the radius within which we must operate while moving load to a data center with higher solar output. We study reduction in the number of panels as we increase the radius by varying degrees. Some values of radii we consider are 100kms, 200kms, 500kms and so on.

3.3.2 Problem Framework

Problem Framework: We model the problem as follows:

Demand and Supply Matrices: We set up the problem as two matrices: one a demand matrix (shown in Table 3.2) and the other a supply matrix (shown in Table 3.1). The values

dcid/time	1	2...	n
1	s_{11}	$s_{12}...$	s_{1n}
2	s_{21}	$s_{22}...$	s_{2n}
3	s_{31}	$s_{32}...$	s_{3n}
..
..
m	s_{m1}	$s_{m2}...$	s_{mn}

Table 3.1: Supply Matrix

in the demand matrix ' l_{ij} ' represent the energy used by the data center at the corresponding time. The values in the supply matrix ' s_{ij} ' represent the solar energy available at that location per panel. Both matrices have ' m ' rows corresponding to data centers and ' n ' columns corresponding to time periods.

Radius of Load Movement: We define the radius of load movement (δ) as the maximum allowable distance we can move load to assign it to another data center.

Neighbors of a data center: We define $N_{i\delta}$ to be the set of all data centers within a radius of δ kms from data center i . Clearly, for an unlimited radius of load assignment, $N_{i\delta}$ is the set of all data centers.

Baseline Panels: We define our baseline panels to be the number of panels we need to serve the IDS load without any load movement. E.g. for net-zero week, for each week, we divide the week's load for the data center by the corresponding week's sum of solar per panel values. We then determine the number of baseline panels by taking the maximum of all the weekly number of panels.

3.4 Algorithms for Solar Provisioning in IDSs

We begin with an LP formulation to solve the solar provisioning problem under performance constraints. Without performance constraints, the number of variables in the original LP formulation becomes very large, resulting in high run-time complexity. So we device a simpler equivalent formulation to solve our solar provisioning problem under no performance constraints. To further reduce runtime complexity for unlimited radius of load

dcid/time	1	2...	n
1	l_{11}	$l_{12}...$	l_{1n}
2	l_{21}	$l_{22}...$	l_{2n}
3	l_{31}	$l_{32}...$	l_{3n}
..
..
m	l_{m1}	$l_{m2}...$	l_{mn}
total load	l_1	$l_2...$	l_n

Table 3.2: Demand Matrix

movement, we also define two heuristic algorithms (MSP and MNP) that run faster while yielding comparable results. The heuristic algorithms are also useful in providing alternative locations for panel provisioning while yielding similar results. All these algorithms are evaluated for their suitability for providing net-zero week, net-zero month and net-zero year solutions.

3.4.1 Optimal LP Formulation

Using the above framework and variables defined in Section 3.3, we formulate an LP problem in order to determine the minimum number of panels we can provision to meet demand, given the solar energy available at various locations. In addition to the above variables, for each data center i , we define variables l_{ijt} to be the load moved from data center i to data center j , at time t , $\forall j \in N_{i\delta}$. Given this setup, we define the LP as shown below. We minimize the total number of solar panels provisioned in the objective function as below:

$$\text{Min: } \sum_{i=1}^m p_i \quad (3.1)$$

We then define constraints as below:

Incoming load should be less than or equal to the solar supply):

$$\text{s.t.: } \sum_{i \in N_{j\delta}} l_{ijt} \leq s_{jt} * p_j, \quad \forall j, t \quad (3.2)$$

Total outgoing load including load moved from the data center to itself should be equal to the starting load:

$$\sum_{j \in N_{i\delta}} l_{ijt} = l_{it}, \quad \forall i, t \quad (3.3)$$

In addition to these constraints, we also have the non-negative constraint for each of the variables defined:

$$l_{ijt} \geq 0, \quad \forall i \in N_{j\delta}, \forall j, t \quad (3.4)$$

$$l_{it} \geq 0, \quad \forall i, t \quad (3.5)$$

$$s_{jt} \geq 0, \quad \forall j, t \quad (3.6)$$

$$p_j \geq 0, \quad \forall j \quad (3.7)$$

$$\delta \geq 0 \quad (3.8)$$

We refer to the above LP formulation as LP_{orig} . For an unlimited radius of load movement, where load can potentially be assigned from a data center to any other data center, the number of l_{ijt} variables, and the number of their associated constraints, becomes very large. For net-zero month, for m data centers, the number of l_{ijt} type variables is $m * m * 12$. For our roughly 1800 data centers and a net-zero month scenario, this number of these variable is a huge number: $1800 * 1800 * 12 = 38,880,000$. Therefore, to keep time and space complexity manageable, we devised a simpler LP formulation for the unlimited radius case. We refer to the simplified LP formulation as LP_{sim} .

For the simpler LP, we define p_i as the number of panels at data center i . l_{it} is the starting load at data center i at time t . s_{it} is the solar energy per panel at data center i at time t . in_{it} is the load moved into data center i at time t . Similarly out_{it} is the load moved out of data center i at time t . Given this setup, we define the LP as shown below.

We minimize the total number of solar panels installed as below:

$$\text{Min: } \sum_{i=1}^m p_i \quad (3.9)$$

Subject to four types of constraints:

Total incoming load minus the outgoing load should be zero:

$$\text{s.t.: } \sum_{i=1}^m in_{it} - \sum_{i=1}^m out_{it} = 0, \quad \forall i, t \quad (3.10)$$

Incoming load should be less than or equal to the solar supply:

$$l_{it} + in_{it} - out_{it} \leq s_{it} * p_i, \quad \forall i, t \quad (3.11)$$

Total outgoing load should be less than or equal to the sum of the starting load and any incoming load:

$$l_{it} + in_{it} - out_{it} \geq 0, \quad \forall i, t \quad (3.12)$$

In addition to these constraints, we also have the non-negative constraint for each of the variables defined:

$$l_{it} \geq 0, \quad \forall i, t \quad (3.13)$$

$$s_{it} \geq 0, \quad \forall i, t \quad (3.14)$$

$$p_i \geq 0, \quad \forall i \quad (3.15)$$

$$in_{it} \geq 0, \quad \forall i, t \quad (3.16)$$

$$out_{it} \geq 0, \quad \forall i, t \quad (3.17)$$

This LP is simpler as it does away with the l_{ijt} type variables that represent load moved from data center i to data center j at time t . Instead it only models load moved in and out of each data center at time t using variables in_{it} and out_{it} . So for the net-zero month case for m data centers for LP_{orig} , where we had to contend with $m * m * 12$ variables, we now only have to work with $m * 12$ variables for the LP_{sim} formulation.

Theorem 1. LP_{orig} for unlimited δ case and LP_{sim} are equivalent.

Proof. In order to prove the above theorem, we prove that the set of feasible solutions of unlimited LP_{orig} and LP_{sim} are the same.

Part I: Proving that a solution of unlimited LP_{orig} is also a solution of LP_{sim} : Firstly, we note that the unlimited LP_{orig} is a more constrained version of LP_{sim} . Therefore, intuitively, any solution that satisfies the unlimited case of LP_{orig} will also be a solution for LP_{sim} . We prove this formally below.

Suppose we have a solution for unlimited LP_{orig} called S_{orig} :

$$S_{orig} = \{l_{ijt} | \forall i, j, t\} \cup \{p_i | \forall i\}$$

Using this solution, we construct another solution S as below:

$$S = \{in_{jt} | \forall j, t\} \cup \{out_{jt} | \forall j, t\} \cup \{p_j | \forall j\}$$

Where we define in_{jt} and out_{jt} in terms of l_{ijt} variables as below:

$$in_{jt} = \sum_{i=1}^m l_{ijt}$$

$$out_{jt} = \sum_{k=1}^m l_{jkt}$$

We now show that S is a feasible solution of LP_{sim} by showing it satisfies all its constraints (3.10 through 3.17):

- *Constraint 3.10 of LP_{sim} :*

$$\begin{aligned} & \sum_{j=1}^m in_{jt} - \sum_{j=1}^m out_{jt} \\ &= \sum_{j=1}^m \sum_{i=1}^m l_{ijt} - \sum_{j=1}^m \sum_{k=1}^m l_{jkt} \end{aligned}$$

Given every outgoing load has a corresponding incoming load, we can cancel all the terms pairwise in the above difference. Therefore,

$$\sum_{j=1}^m in_{jt} - \sum_{j=1}^m out_{jt} = 0$$

- *Constraint 3.11 of LP_{sim} :*

$$\begin{aligned} & l_{jt} + in_{jt} - out_{jt} \\ &= l_{jt} - out_{jt} + in_{jt} \\ &= l_{jt} - \sum_{k=1}^m l_{jkt} + \sum_{i=1}^m l_{ijt} && \text{From definition of } out_{jt} \text{ and } in_{jt} \\ &= 0 + \sum_{i=1}^m l_{ijt} && \text{From Constraint 3.3 of } LP_{orig} \\ &\leq s_{jt} * p_j && \text{From Constraint 3.2 of } LP_{orig} \end{aligned}$$

- *Constraint 3.12 of LP_{sim} :*

$$\begin{aligned}
& l_{jt} + in_{jt} - out_{jt} \\
& = 0 + in_{jt} && \text{Using Constraint 3.3 of } LP_{orig} \\
& = \sum_{i=1}^m l_{ijt} && \text{By definition} \\
& \geq 0 && \text{Using Constraint 3.4 of } LP_{orig}
\end{aligned}$$

- *Non-negativity Constraints 3.13 through 3.17 of LP_{sim} :* All non-negativity constraints also hold. Constraints 3.13 through 3.15 are also constraints in LP_{orig} , so they get ported directly. Constraint 3.16 and 3.17 are true by definition, as they are sums of quantities greater than or equal to zero.

So given S satisfies all the constraints of LP_{sim} , it is also a solution of LP_{sim} . So every solution S_{orig} of LP_{orig} can be reduced to a feasible solution S of LP_{sim} .

Part II: Proving that a solution of LP_{sim} is also a solution of LP_{orig} : Suppose we have a solution S_{sim} for LP_{sim} as defined below:

$$S_{sim} = \{in_{jt} | \forall j, t\} \cup \{out_{jt} | \forall j, t\} \cup \{p_j | \forall j\}$$

Using this solution, we construct another solution S below by defining l_{ijt} values in terms of in_{jt} and out_{jt} values:

$$S = \{l_{ijt} | \forall i, j, t\} \cup \{p_i | \forall i\}$$

We first consider the net inflow and out flow for each location, given by the following difference:

$$in_{jt} - out_{jt} \forall j, t$$

Respecting these net inflows and outflows, we define our l_{ijt} by matching inflows with outflows, ensuring we only pick non-negative values for each l_{ijt} . Note this matching can

always be done because constraint 3.10 is satisfied, meaning net inflow and net outflow in the system are the same. We note that multiple such sets of l_{ijt} values can satisfy the condition, but we only need to pick one of them to prove the result. We also note that for each location i , l_{iit} is counted both as incoming load and outgoing load. With this, we can see that the starting load in a location is the sum total of the outgoing load. Also the net ending load at a location is the sum of the incoming load:

$$in_{jt} = \sum_{i=1}^m l_{ijt} \quad (3.18)$$

$$out_{jt} = \sum_{k=1}^m l_{jkt} \quad (3.19)$$

$$l_{jt} = out_{jt} \quad (3.20)$$

With this definition of l_{ijt} variables, we show that all the constraints of LP_{orig} are satisfied:

- *Constraint 3.2 of LP_{orig} :*

$$\begin{aligned} & \sum_{i=1}^m l_{ijt} \\ &= in_{jt} + 0 && \text{Using equation 3.18} \\ &= in_{jt} + l_{jt} - out_{jt} && \text{Using equation 3.20 and expanding 0} \\ &\leq s_{jt} * p_j && \text{Using constraint 3.11 of } LP_{sim} \end{aligned}$$

- *Constraint 3.3 of LP_{orig} :*

$$\sum_{k=1}^m l_{jkt} = l_{jt}, \forall j, t$$

This constraint is satisfied because of how we defined our l_{ijt} variables (as shown in equations 3.19 and 3.20).

- *Non-negativity constraints 3.4 through 3.8 of LP_{orig} :* Constraint 3.4 is satisfied by the way l_{ijt} were chosen. Constraints 3.5 through 3.7 can be directly ported from LP_{sim} . Constraint 3.8 is also satisfied as δ is unlimited in this case.

So given S satisfies all the constraints of LP_{orig} , it is also a solution of LP_{orig} . So every solution S_{sim} of LP_{sim} can be reduced to a feasible solution S of LP_{orig} .

Therefore, given the proofs of Part I and Part II above, we prove that the two LP formulations LP_{orig} and LP_{sim} are equivalent.

□

3.4.2 Greedy Heuristic Algorithms

We describe below our heuristic algorithms that are inspired at a high level by greedy approximation algorithms to the set-covering problem [18]. We loosely consider the load to be served as the set to be covered. The different amounts of load we can serve using energy generated from solar panels at various locations are like the subsets that can cover the original set.

3.4.2.1 Max Solar Per Panel Heuristic (MSP)

We now define a greedy heuristic algorithm that runs faster than the LP, performs comparably, and offers a set of alternative locations for panel provisioning. We use the same problem framework with the demand and supply matrices that we defined in Section 3.3. In order to minimize the number of panels, we note that we need to assign as much load as we can to a location that has the highest solar output. This would help us to cover the maximum load with the minimum number of panels for a given time slot. We greedily pick the maximum solar per panel location across time and space (i.e. across all data centers), and assign the entire load for the time period to that location. Using the solar per panel value and the load, we determine the number of panels to place at that location. Once we install panels at a location, these panels can then be used to serve demand for other time periods as well, so we accordingly adjust the demand values to reflect the extra supply for all other time periods as well. We continue to place panels in this way until we satisfy the entire demand in all time periods. The correctness of this algorithm is clear due to fact that the

DCID/Time	1	2	3
dc1	3	5	3
dc2	3	4	4
Total load	180	100	600

Table 3.3: Counter example for MSP showing the algorithm is not globally optimal

process continues until the entire load is covered. Pseudocode for this algorithm is detailed in Algorithm 1.

This is a greedy algorithm that tries to do the best for each time slot. It does not necessarily do the best globally for all time slots. This can be seen with the following toy example. Suppose we have two data centers and two time slots, with load and solar per panel values as shown in the Table 3.3. If we assign load according to our algorithm, we would first assign 100 units to dc1 with solar per panel value 5, resulting in 20 panels in dc1. We would then adjust loads, and assign the left over 540 units to dc2 in time slot 3, resulting in 135 panels in dc2. This would give us a total of 155 panels across all time periods. However, instead of the above assignments, we could serve all the load with assigning 150 panels to dc2 in time slot 3.

Algorithm 1 MSP Heuristic Pseudocode

```

function SPHEURISTIC( )
  time  $\leftarrow [t_1, t_2, \dots, t_n]$  ▷ time periods
  spp  $\leftarrow [s_{11}, s_{12}, \dots, s_{mn}]$  ▷ solar output
  load  $\leftarrow [l_1, l_2, \dots, l_n]$  ▷ load for time period
  provpanels  $\leftarrow []$  ▷ provisioned panels
  for  $t_y$  in time do
     $s_{xy} \leftarrow \min s_{ij}$  s.t.  $s_{ij} \in spp$  ▷ pick min solar
     $p_{xy} \leftarrow l_y / s_{xy}$  ▷ assign panels
    provpanels  $\leftarrow provpanels \cup [p_{xy}]$  ▷ add to provisioned panels
    for  $i$  in  $[1, 2, \dots, m]$  do
       $l_i \leftarrow |l_i - l_y|$  ▷ adjust other loads
    load  $\leftarrow load - l_y$  ▷ delete assigned load
  return provpanels

```

dcid/time	1	2...	n
1	p_{11}	$p_{12}\dots$	p_{1n}
2	p_{21}	$p_{22}\dots$	p_{2n}
3	p_{31}	$p_{32}\dots$	p_{3n}
..
..
m	p_{m1}	$p_{m2}\dots$	p_{mn}

Table 3.4: Number of Panels Matrix

3.4.2.2 Minimum Number of Panels Heuristic (MNP)

We now describe our second heuristic algorithm. The basic structure of this algorithm is the same as the ‘MSP Heuristic’ algorithm, except we now use a different heuristic to make a decision on where to put panels. We first determine the number of panels for each location for each time period, by dividing the load for the time period for all locations, by the solar per panel for the corresponding time and location. This gives us the ‘Number of Panels Matrix’ shown in Table 3.4. We then pick the lowest number of panels value and install those many panels at the corresponding location and time period. Like before, once any panels are installed at a location, they are also available for other time slots. So we accordingly adjust the demand to reflect the extra supply. We recompute the number of panels matrix for the adjusted loads, and start over. We do this exercise until all the demand is met. The correctness of this algorithm is clear due to fact that the process continues until the entire load is covered. Pseudocode for this algorithm is detailed in Algorithm 2.

Like the MSP, the MNP is also greedy heuristic algorithm that tries to do the best for each time slot. It does not necessarily do the best globally for all time slots. This can be seen using the same counter example we used for the MSP Heuristic shown in Table 3.3. The MNP Heuristic would yield 165 panels across all time periods. However, we could serve all the load with assigning 150 panels to dc2 in time slot 3.

Algorithm 2 MNP Heuristic Pseudocode

```
function NPHEURISTIC( )  
  time  $\leftarrow [t_1, t_2, \dots, t_n]$  ▷ time periods  
  spp  $\leftarrow [s_{11}, s_{12}, \dots, s_{mn}]$  ▷ solar output  
  load  $\leftarrow [l_1, l_2, \dots, l_n]$  ▷ load for time period  
  origpanels  $\leftarrow []$  ▷ original panels  
  provpanels  $\leftarrow []$  ▷ provisioned panels  
  for sij in spp do  
    opij  $\leftarrow l_i/s_{ij}$  ▷ determine original num panels  
    origpanels  $\leftarrow \text{origpanels} \cup [op_{ij}]$  ▷ add to original panels  
  for ty in time do  
    opxy  $\leftarrow \min op_{ij}$  s.t. opij  $\in$  origpanels ▷ pick min panels  
    pxy  $\leftarrow l_y/s_{xy}$  ▷ assign panels  
    provpanels  $\leftarrow \text{provpanels} \cup [p_{xy}]$  ▷ add to provisioned panels  
    for i in [1, 2, ..., m] do  
      li  $\leftarrow |l_i - l_y|$  ▷ adjust other loads  
    load  $\leftarrow \text{load} - l_y$  ▷ delete assigned load  
    time  $\leftarrow \text{time} - t_y$  ▷ delete time column  
    for sij in spp do  
      opij  $\leftarrow l_i/s_{ij}$  ▷ determine num panels  
      origpanels  $\leftarrow \text{origpanels} \cup [op_{ij}]$  ▷ add to panels  
return provpanels
```

Parameter	Value
Loss %	14
System Capacity	0.275 kW
Module Type	Standard
Timeframe	Hourly
Azimuth	180 deg for northern hemisphere and 0 for southern
Tilt	Absolute value of latitude
Dataset	'TMY2' for US Locations and 'Intl' for others

Table 3.5: Parameters for PVWatts Data

3.5 Experimental Methodology

We conduct experiments using an extensive Akamai load trace spanning a month. The trace consists of load information from 100,592 servers in over 724 global datacenter locations. The dataset includes load, requests served, and bytes served by each server every five minutes over a month-long trace. Further, the trace has detailed information about every data center, including the number of deployed servers, total server capacity, and the location of the data center including its latitude, longitude, city, state, and country. After excluding locations without solar data and data cleaning, we could still cover 93.4% of the load.

For solar energy data, we use the PVWatts [52] hourly data of AC energy generation from solar radiation for a year. Assuming the power rating for solar panels is between 200 watts and 350 watts [25], we take an average value of 275 watts as the power rating per panel. Therefore, we use the system capacity as the 0.275 kW for pvwatts in order to get the output generated by a single panel. For simplification, for all other required parameters, we use the values listed under 'Default Values' on page 3 in the PVWatts version 5 manual [20]. The required parameters used for downloading pvwatts data are detailed in Table 3.5.

The load data has 5-minute readings, whereas the solar data is hourly. So we make an assumption that solar data does not change much during the hour and used an hour's reading for each of the five minutes that fall within that hour. Also, we have the solar data for the year, but we have the load trace for one month only. We assume that the load pattern for the CDN repeats monthly for the year. For each five minute reading, we convert the solar

AC output (in watts) into energy (in joules) by multiplying by the number of seconds in five minutes. Similarly, we convert the load into energy drawn (in joules) by multiplying the power consumed (in watts) by servers for each five minute interval by the number of seconds in five minutes.

The load represents energy demand and the solar radiation per panel represents energy supply. In order to optimize the number of panels, our algorithms take into account the amount of solar energy available in different locations at different time periods.

Through our experiments, we study three different scenarios under which we move load to leverage solar: The first scenario enforces no performance constraints and allows unrestricted movement of load to take advantage of high levels of solar in different global locations. The second scenario allows unrestricted load movement, however, constraints the locations for panel provisioning to only be the top k locations sorted by the number of servers. The last scenario restricts load movement within a certain radius, and we consider a number of such radii. In addition, for each scenario above, we repeat the study for net-zero week, net-zero month, and net-zero year.

With the above setup, our experimental evaluation seeks to answer the following questions for each of the three scenarios above, for each net-zero time period:

- How much of a reduction can we see in the number of panels when compared to not moving load anywhere to take advantage of solar?
- Which net-zero time period requires the most panels and why?
- Which net-zero time period benefits the most from load shifting?
- Which global locations are picked for solar provisioning?
- How do the algorithms compare in their ability to reduce the number of panels?
- For the second (top k) scenario, how do the results change with different radii?
- For the top k scenario, how does the number of locations selected vary with k ?

- For the last scenario with restricted load movement, how do the above results vary with different radii?
- For the last scenario, how does the number of locations selected vary with different radii of load movement?

3.6 Empirical Results

The following paragraphs describe our results for scenarios when we allow unrestricted load movement to take advantage of solar (*Without Performance Constraints*) and when we restrict the radius of load movement (*With Performance Constraints*).

3.6.1 Without Performance Constraints

The goal of this experiment was to study the maximum reduction in solar panels that we can achieve by allowing unrestricted load movement between data centers. The paragraphs below discuss our findings in detail.

3.6.1.1 Reduction in Number of Panels

As base comparison, for each data center and each net-zero time period, we first calculate the number of panels we would need if we did not do any load movement (as described in section 3.3.2). We then run LP_{sim} and the two heuristic algorithms (MSP and NP) for net-zero week, net-zero month, and net-zero year. We normalize the number of panels in for each algorithm, for each net-zero time period using the corresponding original number of basepanels. Our results are shown in Figure 3.1.

Our main observations are as below:

- *Load movement helps dramatically:* We see a significant decrease in the number of panels across time periods for our optimal and heuristic algorithms. For net-zero year, the total number of panels needed to serve the load decrease by 36% for all algorithms. For net-zero month, the MNP heuristic algorithm shows a decrease of

about 66.94%, while the MSP heuristic shows a decrease of 67.03%. The LP performs slightly better and shows a decrease of almost 68%. For net-zero week, once again the heuristic algorithms perform similarly and decrease panels by between about 71% to about 74%. The LP performs significantly better and reduces the number of panels by almost 82%.

- *Number of panels vary inversely with the size of the net-zero time period:* The number of panels provisioned is highest for net-zero week, followed by net-zero month, followed by net-zero year. This is intuitive given for net-zero year we are averaging over a larger time period than for net-zero month or net-zero week. Similarly, for net-zero month we are averaging over a larger time period than net-zero week. So we are moving from a less restricted space to a more restricted space as we go from year, to month to week. Therefore, the set of feasible solutions for the more restrictive net-zero week, is also a solution for net-zero month and net-zero year. Similarly, the set of feasible solutions for net-zero month is also a solution for net-zero year. Given the above, the number of panels can only decrease or remain the same as we move from net-zero week to net-zero month to net-zero year.
- *Optimal LP shows excellent results for all net-zero time periods:* The optimal LP shows a significant reduction in the number of panels, and as expected, performs better than the heuristic algorithms. We see a reduction of nearly 82% for net-zero week, more than 83% for net-zero month, and more than 84% for net-zero year . With the LP, the difference between the number of panels across time periods narrows significantly compared to when no load is moved.
- *Heuristic algorithms are well-behaved and perform comparably:* The heuristic algorithms behave well and also yield a significant reduction in the number of panels. The MSP heuristic performs better than the MNP heuristic, yielding a larger reduction

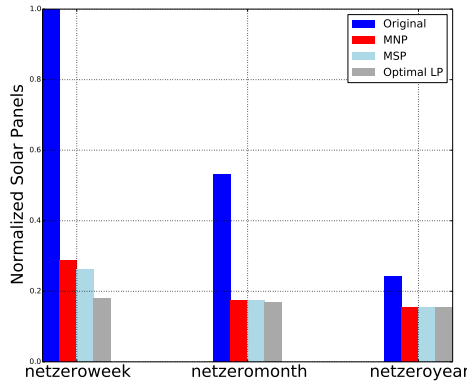


Figure 3.1: Plot shows that number of panels provisioned is inversely proportional to the time period over which we aim to be net-zero

for net-zero week. For net-zero month and net-zero year, both algorithms performs almost equally well.

3.6.1.2 Location Choices for Different Algorithms

In this section, we discuss why the heuristic and optimal algorithms pick certain locations for net-zero year, net-zero month and net-zero week under unrestricted load movement. For net-zero year, all algorithms favor the location that has the maximum total annual solar output, and place all panels in that location. For the locations we considered, Arequipa, Peru was the location that topped the list for annual solar output. Therefore, as Table 3.6 shows, all the algorithms assigned the sum total of the load to Arequipa.

Location	MSP	MNP	LP
AREQUIPA, Peru, South America	100	100	100

Table 3.6: % Panels by location for net-zero year without performance constraints

For net-zero month, the percentage break-up by locations is detailed in Table 3.7. We see that the algorithms tend to favor locations that have consistently high monthly solar output, with low variance. If we normalize monthly solar output values based on the max of all the monthly solar output values across all considered locations, we find that Arequipa

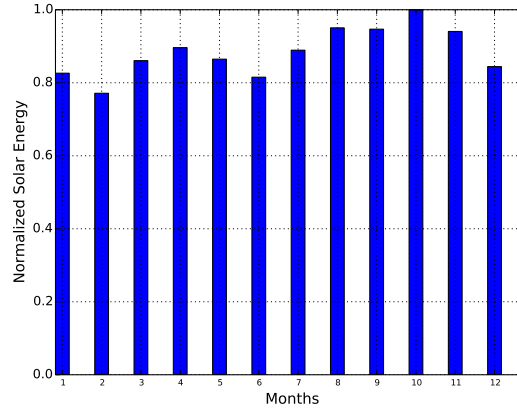


Figure 3.2: Plot shows that Arequipa, Peru has a high solar output consistently across all the months of the year

performs quite well. As Figure 3.2 shows, the normalized monthly solar never falls below the 80% level, except slightly for the second month. Given the above, we observe that LP favors Arequipa and places over 96% panels there. The heuristic algorithms also place the majority of their panels (over 80%) in Arequipa.

Location	MSP	MNP	LP
AREQUIPA, Peru, South America	80.05	84.01	96.07
ALBUQUERQUE, NM, United States, North America	1.97	2.26	0
PAROW, South Africa	14.23	5.43	0
JERUSALEM, Israel	3.75	1.57	0
YELLOWKNIFE, Canada	0	2.92	0
MONTEREY, CA, United States	0	3.81	0
PERTH, Australia	0	0	3.93

Table 3.7: % Panels by location for net-zero month without performance constraints

For net-zero week, the percentage break-up of the number of panels by location is detailed in Table 3.8. Locations that have a high weekly solar output tend to get picked. Figure 3.3 shows the normalized weekly solar output for Arequipa. We observe that for most weeks, Arequipa has a higher than 70% output. However, there are a few weeks where Arequipa does not do so well (e.g. for week 10 the output falls below 60%). The LP assigns more than half the panels to Arequipa. The heuristic algorithms, however, pick Winnipeg, Canada for assigning over 40% of panels. Winnipeg is not one of the top locations for annual

Location	MSP	MNP	LP
REGINA, Canada	4.09	1.54	0
AREQUIPA, Peru, South America	27.06	5.04	50.34
SANTIAGO, Chile	8.16	7.66	0
PAROW, South Africa	7.58	9.80	0
WINNIPEG, Canada	47.05	43.22	0
CANBERRA, Australia	6.05	0	0.31
LAGRANDE, OR, United States	0	0.53	0
BEND, OR, United States	0	0.61	0
LISBON, Portugal	0	0.36	0
RENO, NV, United States	0	1.62	0
YELLOWKNIFE, NT, Canada	0	4.14	0
JERUSALEM, Israel	0	0.03	0
EL PASO, TX, United States	0	0.18	0
SUDBURY, ON, Canada	0	0.14	0
BUENOS AIRES, Argentina	0	0.39	0
SAN LUIS OBISPO, CA, United States	0	1.21	0
CANBERRA, Australia	0	7.04	0
LA PAZ, Bolivia	0	0.85	0
THEBARTON, Australia	0	0.39	0
TUCSON, AZ, United States	0	0.91	0
SAINT GEORGE, UT, United States	0	0.49	0
MONTEREY, CA, United States	0	12.51	0
ALBUQUERQUE, NM, United States	0	1.66	0
PERTH, Australia	0	0	5.17
HAYS, KS, United States	0	0	7.06
ALAMOGORDO, NM, United States	0	0	14.78
PRETORIA, South Africa	0	0	14.62
CEDAR CITY, UT, United States	0	0	7.73

Table 3.8: % Panels by location for net-zero week without performance constraints

solar output. However, it has extremely high solar output during one of its weeks. From this analysis, we learn that the LP tends to pick more robust locations that have consistently high solar output, where as the heuristic algorithms may pick locations that have a few weeks where their solar output is the maximum of any location.

With unrestricted load movement, observe that for all the algorithms, load is moved to locations that are high in solar output for the time period under consideration. However, with these choices we find that load could end up in remote locations, resulting in high levels

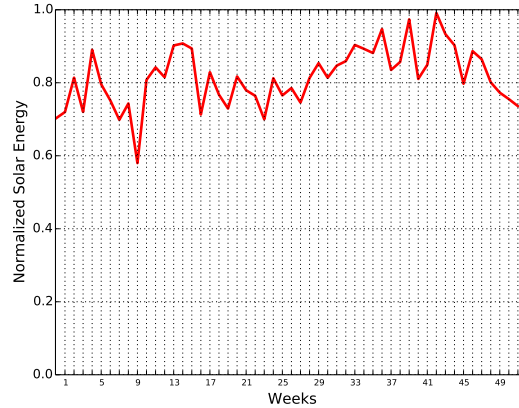


Figure 3.3: Plot shows that Arequipa, Peru has a high solar output for most weeks of the year, except a few where the plot dips

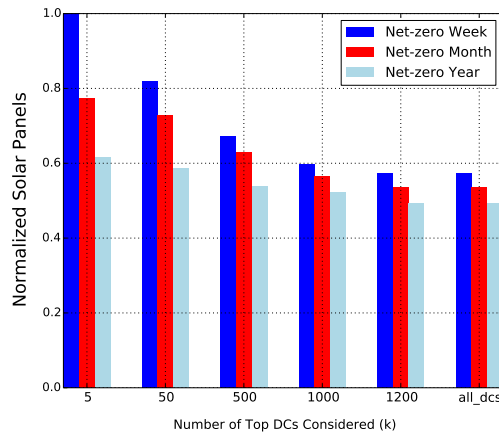


Figure 3.4: Number of panels provisioned are highest for net-zero week, followed by net-zero month and then net-zero year

of latency. To remedy this problem, we try to restrict solar panels to locations that are not remote and have a large amount of load to start with.

3.6.1.3 Restricting Panels to Top K Data Centers

Given servers need to be proximal to users, we use the number of servers in a data center as the proxy for data centers that are large and are located in non-remote places with large populations. Therefore, we allow unrestricted load movement, but restrict panel provisioning to top k locations sorted by the number of servers.

Discussion on number of panels: We analyze of the change in the number of panels if we restrict our panel provisioning to only the top k data centers. We normalize the number of panels using the maximum value in the set (i.e. number of panels for net-zero week for top 5 data centers). Figure 3.4 shows the change in the number of panels across different values of k . We list our observations below:

- *Number of panels provisioned varies inversely with k :* First of all, we see that the number of panels provisioned increases when we restrict ourselves to fewer locations. This is intuitive considering that we are operating with more constraints, and therefore are not able to extract as much reduction from solar output as we could in an unrestricted setting. The larger the k , the more locations are in play for extracting solar savings.
- *Number of panels vary inversely with the size of the net-zero time window:* Once again, we see that the number of panels provisioned is the most for net-zero week, followed by net-zero month, and finally net-zero year. This trend is preserved across different values of k . This is intuitive given we are averaging over a larger time period for net-zero year as compared to net-zero month. In the case of a net-zero year, we must match demand with supply over the entire year. For net-zero month we must match demand with supply for *each* month, however, low our supply maybe and however high our demand may be for various months. Therefore, we must satisfy our net-zero condition for the 'worst' month in our list. Similarly, we must satisfy the net-zero week condition for the worst week on our list. Therefore, the number of panels increase as we move from net-zero year, to net-zero month, to net-zero week.
- *Sensitivity to change in k is inversely proportional to size of net-zero window:* The smaller the time window, the greater the sensitivity to change in k . The net-zero week bars show a steeper decline when we move from smaller value of k to larger values of k , as compared to the net-zero month bars.

- *k=500 balances both objectives well*: For $k=500$, we see that the number of panels are very close to the unrestricted panel provisioning case. Therefore, restricting to the top 500 data centers is a good middle point for achieving moderate number of panels installed at non-remote locations.

Discussion on location choices under top k restrictions: As expected, with top k restrictions, we find that the locations selected for the majority of panels with smaller values of k tend to be larger cities. E.g. for $k=5$ net-zero year selects Dallas, TX versus for $k=1200$, the location picked is Arequipa, Peru. Similarly, for net-zero month, for $k=5$, the location picked is Dallas, TX again and for $k=1200$, Arequipa and Perth are picked. For net-zero week, for $k=5$, Atlanta is picked, and for $k=1200$, we see almost half of the panels provisioned in Arequipa. Tables 3.9, 3.10 and 3.11 show the details of the locations selected.

K	Location	Percentage Panels
5	DALLAS, TX, United States, North America	100.0
50	LOSANGELES, CA, United States, North America	100.0
500	SCOTTSDALE, AZ, United States, North America	100.0
1000	HENDERSON, NV, United States, North America	100.0
1200	AREQUIPA, Peru, South America	100.0

Table 3.9: Locations under Top K Restrictions for Net-zero Year

K	Location	Percentage Panels
5	DALLAS, TX, United States, North America	100.0
50	MIAMI, FL, United States, North America	88.83
	LOSANGELES, CA, United States, North America	11.17
500	SCOTTSDALE, AZ, United States, North America	61.08
	AUCKLAND, New Zealand, Oceania	34.
	SYDNEY, NSW, Australia, Oceania	4.37
1000	RANDBURG, South Africa, Africa	51.80
	LASVEGAS, NV, United States, North America	31.88
	PERTH, WA, Australia, Oceania	16.32
1200	AREQUIPA, Peru, South America	96.07
	PERTH, Australia, Oceania	3.93

Table 3.10: Locations under Top K Restrictions for Net-zero Month

K	Location	Percentage Panels
5	ATLANTA, GA, United States, North America	100.0
50	DALLAS, TX, United States, North America	50.4
	LOSANGELES, CA, United States, North America	49.66
500	RIODEJANEIRO, RJ, Brazil, South America	31.36
	SCOTTSDALE, AZ, United States, North America	21.01
	SANTOS, SP, Brazil, South America	13.14
	LOSANGELES, CA, United States, North America	11.88
	AUCKLAND, New Zealand, Oceania	9.55
	CAIRO, Egypt, Africa	8.62
	SYDNEY, NSW, Australia, Oceania	3.06
	DENVER, CO, United States, North America	1.38
1000	DUBAI, United Arab Emirates, Asia	39.40
	PERTH, Australia, Oceania	19.46
	RANDBURG, South Africa, Africa	16.49
	AMMAN, Jordan, Asia	10.08
	LASVEGAS, NV, United States, North America	7.07
	BUENOSAIRES, Argentina, South America	3.27
	ADELAIDE, SA, Australia, Oceania	2.15
	BRISBANE, QLD, Australia, Oceania	1.58
	SCOTTSDALE, AZ, United States, North America	0.50
1200	AREQUIPA, Peru, South America	50.20
	ELPASO, TX, United States, North America	14.41
	RANDBURG, South Africa, Africa	11.80
	SAINTGEORGE, UT, United States, North America	11.75
	PERTH, WA, Australia, Oceania	6.87
	LASVEGAS, NV, United States, North America	2.70
	CANBERRA, ACT, Australia, Oceania	2.28

Table 3.11: Locations under Top K Restrictions for Net-zero Week

3.6.2 With Performance Constraints

The goal of this experiment was to study the impact of load movement within a radius on the reduction in the number of panels when compared to the two extremes of unrestricted load movement and no load movement at all. For this experiment, we selected a set of values of radii and generated LPs consistent with those radii and with different net-zero time periods.

3.6.2.1 Discussion on the Number of Panels

In Figure 3.5, we plot the normalized number of panels for each of the net-zero time periods for different radii. We list our observations below:

- *Load movement to larger radii helps dramatically:* We see a huge reduction in the number of panels as we move from a smaller radius to larger radius.
- *Number of panels is inversely proportional to size of net-zero time window:* Once again, we see that net-zero week has the largest number of panels, followed by net-zero month, and then net-zero year. As explained in section 3.6.1, this is due to averaging over larger time periods for net-zero year and net-zero month when compared to the net-zero week. It is also because for net-zero week, we aim to be net-zero week for all the weeks of the year - including the ‘worst’ week that has the lowest solar output.
- *Sensitivity to change in radius is most pronounced for shorter net-zero window:* Figure 3.6 shows the percentage decrease in the number of panels for different radii and net-zero timer periods when compared to no load movement. Overall, we observe that when we enforce performance constraints, we see different degrees of reduction for different net-zero periods. The curve is the steepest for netzero week, followed by netzero month and then netzero year. This means that we get the greatest and fastest benefit from using locations with high solar output in the case of netzero week. The dotted horizontal lines represent the maximum reduction we can hope to achieve if we allow unlimited radius load movement. For netzero week, we see that even with a maximum radius of 200kms, we can extract a 31% reduction in the number of panels. For netzero month, with a radius of 500kms, we see a reduction of over 27%. With a radius of 1500kms, we can cut down the number of panels by over half with a reduction of 53%. For netzero year, the reductions are significant, but not as pronounced. With a radius of 500kms, we can decrease the number of panels by nearly 10%.

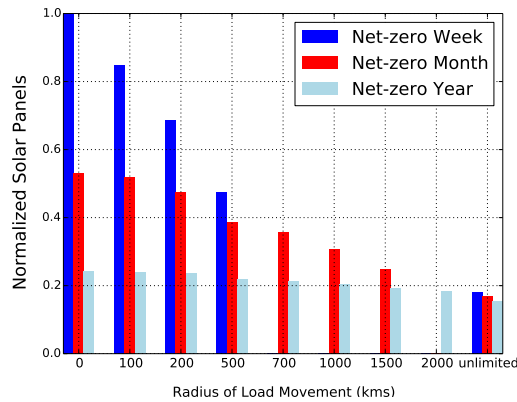


Figure 3.5: Plot shows that net-zero week has the largest number of panels for any radius, then net-zero month, and finally net-zero year

3.6.2.2 Location Choices for Different Algorithms

We study location choices and plot the number of locations across different radii for different net-zero time periods. Our main observations are:

- Number of locations decrease with increase in radius:* Figure 3.7 shows that with an increase in the radius of load movement, the number of locations where solar panels are allocated decreases for each net-zero time period. This is because as the radius increases, load converges to locations that are globally high for solar output. Figure 3.9 shows the locations that are chosen for various values of max radius for net-zero month, on a world map. For net-zero year, for smaller radii, we see that the locations are local picks with higher solar. As we proceed to higher and higher radii, the locations picked are globally high for solar for that time period. We see the locations shrink and converge to the hubs for solar generation.
- Number of locations is inversely proportional to the size of net-zero time period:* Figure 3.7 also shows that the number of locations are the maximum for net-zero week followed by net-zero month, and then net-zero year. Net-zero month and net-zero year are closer in the number of locations they pick. Figure 3.8 shows the distribution of panels for a radius of 500kms for different net-zero time periods. We observe that

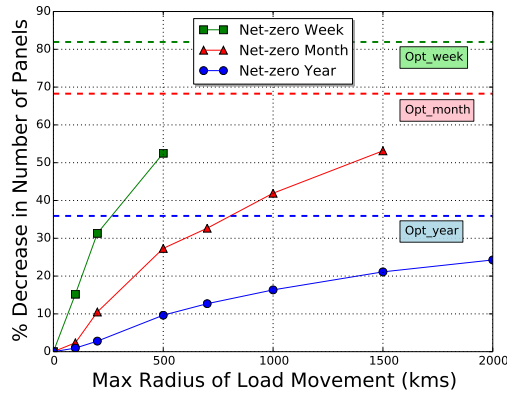


Figure 3.6: Plot shows % decrease in number of solar panels as radius of load movement is increased. Dotted lines labeled ‘Opt_week’, ‘Opt_month’, and ‘Opt_year’ show the maximum decrease we can hope to have with an unlimited radius.

for all the net-zero time periods, panels are fairly evenly distributed with a few high peaks, and the highest peak for each time period lies between 12% and 16%.

3.7 Implications for IDS Design

Overall, our study shows that load movement helps in reduction of solar panels dramatically. The shorter the net-zero time window, the larger the number of panels the IDS needs to achieve net-zero state for each such time period over the course of a year. In addition, for shorter net-zero time periods, the number of locations where panels need to be installed for the IDS increases. IDSs can also achieve significant reduction in the number of panels by moving load within restricted radii to minimize latency. In addition, IDSs can achieve a significant reduction in the number of panels even if they restrict panel provisioning to the larger data center locations. However, in general, restricting panels within a radius or to certain data centers leads to a lesser reduction in the number of panels and an increase in the number of locations where panels are provisioned. Our solution can also be used to restrict panel provisioning to other locations using other criteria, and to study the impact of such a restriction on the reduction in the number of panels.

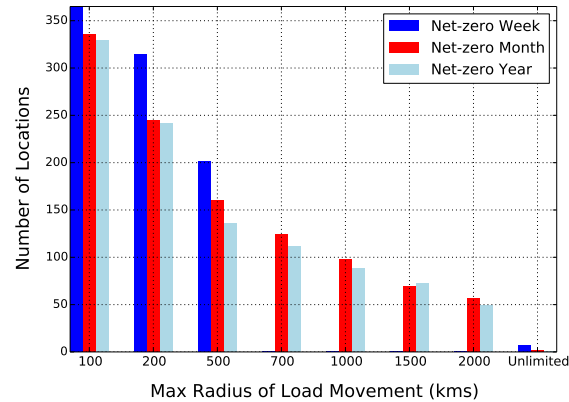


Figure 3.7: Plot shows that the number of locations where panels are allocated decrease as we increase the radius of load movement. This is because the load converges to global locations with high solar output

3.8 Related Work

Recently, a lot of work has been done in the area of renewables for data centers. Work has been done on job scheduling within a data center based on predicted solar and brown energy prices [29] [28]. Previous work has also modeled the potential of using renewable energy for data centers located in colder locations [62], while [40] propose a solution for data center expansion using modular solar panels and distributed battery systems to have near-zero environmental impact. While this work takes advantage of renewables to reduce energy consumption, it does not deal with optimal provisioning of solar panels for an existing global IDS. Moving load across data centers to increase the use of renewables has also been studied before. Studies have also been done [47] [46] on how and to what extent geo-graphical load balancing can encourage use of renewable energy and reduce use of brown energy. Their distributed algorithm offers significant savings in cost (defined by linear combination of energy cost and delay cost). Prior work has also studied green solutions that control user traffic and direct to different data center locations based on changes workload and carbon footprint [27]. However, all these works [47] [46] [27] focus on load balancing and request routing rather than provisioning of renewables. Previous work has also looked into providing a solution for selecting sites for and provisioning green data centers using

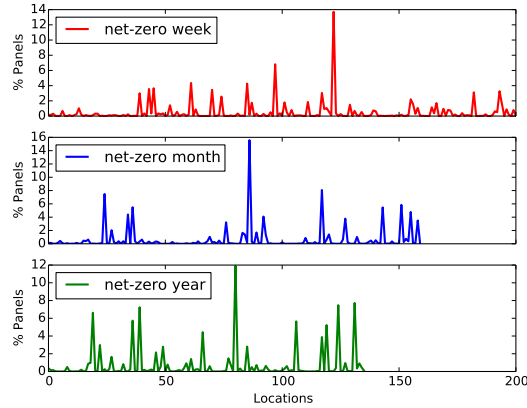
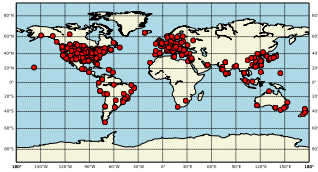
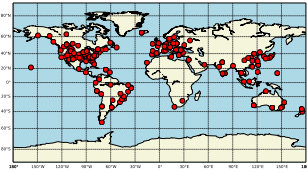


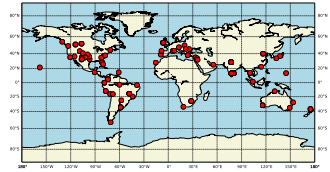
Figure 3.8: Distribution of panels for 500kms for different net-zero time periods showing that the number of locations is largest for net-zero week, then for net-zero month, and finally for net-zero year



a) Max radius = 100



(b) Max radius = 500



(c) Max radius = 1500

Figure 3.9: Locations where the LP with performance constraints send the load to for net-zero month

a follow-the-renewables approach [13]. However, their work focuses on setting up a data centers from scratch, where as our data center locations are given. In addition, they base the placement of their datacenters partially on a combination of availability of solar and wind energy. In contrast, our decisions are solely driven by the availability of solar. We also study the impact on panel provisioning of moving load within radii of different distances around each datacenter.

3.9 Conclusions

In this chapter we studied the optimal solar provisioning of solar panels for net-zero IDSs. Using our heuristic and optimal algorithms, we are able to significantly reduce the

number of solar panels needed for serving load in our datacenters. Specifically, we see a decrease of close to 36% in the total number of panels for both heuristic and optimal LP algorithms for netzeroyear. For net-zero month, we see a decrease of about 67% for the heuristic algorithms and 68% for the LP. For netzeroweek, we see a decrease of about 71% to about 74% for the heuristic algorithms and almost 82% for the LP. We also observed that using our LP algorithm, we can achieve net-zero week in nearly the same number of panels as we need to achieve net-zero month and net-zero year. If we allow unlimited load movement, but restrict panel provisioning to topk locations, we can achieve significant reduction in the number of panels. Allowing only top 500 locations to be in play, we can achieve net-zero year with less than 9% increase in the number of panels, net-zero month and net-zero week with less than 18% increase. We also show that if we restrict the radius of load movement, we can achieve significant reduction in the number of panels for all net-zero time periods even with relatively small radii. For netzero week, we see that even with a maximum radius of 200kms, we can extract a 31% reduction in the number of panels. For netzero month, with a radius of 500kms, we see a reduction of over 27%,and for net-zero year, a reduction of nearly 10%. In conclusion, we demonstrated that by leveraging locations with high solar output, we can significantly reduce the number of panels needed to serve load and achieve net-zero status over different time periods. This reduction in the number of solar panels translates to savings in capital and operating expenses for data centers and makes the transition to renewables that much easier for existing IDSs.

CHAPTER 4

OPEN AIR COOLING FOR GREENING INTERNET-SCALE DISTRIBUTED SYSTEMS

Open Air Cooling (OAC) is a technology that has gained traction within data centers. OAC also sometimes referred to as free cooling, uses outside air to cool servers whenever the climate permits, e.g. when the outside air is sufficiently cool or dry. OAC can decrease, or even eliminate, the use of chillers used to chill the air for cooling the servers. Service providers who employ large data centers such as Facebook and Google have begun to use OAC, in part by building new data centers in carefully chosen (cold) locations where the climate permits the outside air to be used to cool the data center for the majority of the year.

While existing techniques to reduce energy consumption in data centers yield significant cost benefits, they only address the energy costs of powering the servers and do not *directly* address the energy cost of cooling them. In this part of the thesis, we focus explicitly on the complementary problem of reduction in cooling costs using *renewable open air cooling (OAC)*.

A recent study of data center energy consumption [56] showed that servers and cooling consumed 56% and 30% of the total energy respectively, while power conditioning (8%), networks (5%) and lighting (1%) accounted for the rest. Thus, most of the energy consumed by a data center is spent in powering servers or cooling them; we refer to these components as *server energy* and *cooling energy*, respectively. Since cooling energy is a significant portion of the total energy consumption, we examine the potential for employing two new cooling technologies to reduce either the energy usage or the energy cost incurred by an IDS, or both.

In this chapter, our focus is on understanding the efficacy of using OAC for IDSs. To our knowledge, OAC has not been studied in an IDS context that is distinctive for the following reasons. IDSs such as CDNs have two defining characteristics: *a global deployment* of servers in multiple data centers around the world, and a *replication* of services across these data centers. The global deployment is often driven by the need for an IDS to have servers “proximal” to the end-users. For instance, Akamai’s CDN is deployed in hundreds of data centers in over 100 countries around the world, with users accessing content from servers in “proximal” data centers [53]. A corollary of this deployment model is that it is not possible for IDSs to deploy *only* in places where weather is cold most of the year, or where electricity is cheap. They need to be deployed near where the users are. However, IDSs often replicate their services across their data centers, so that the workload of serving users can be easily shifted from one data center to another, albeit with a potential for performance degradation. These two characteristics provide an IDS the flexibility to move its workload across data centers to exploit climatic variations to optimize the use of OAC, a flexibility that services employing a single or a few data centers do not possess. The energy cost also varies across locations and across time. Our algorithms orchestrate the movement of load (i.e, load balancing) to decrease an IDS’s cooling costs.

4.1 Contributions

- *Determining OAC Potential for Global IDSs:* To the best of our knowledge, this is the first study that researches OAC potential for global IDSs.
- *Simple Greedy Algorithm:* We develop a simple greedy algorithm for exploiting OAC globally. We design this algorithm in a way that allows us to enforce performance constraints by restricting the radius of load movement.
- *Extensive Trace-based Evaluation:* We evaluate OAC using extensive load traces from the world’s largest CDN. The traces were collected from Akamai’s CDN every five

minutes for the period of a month from over 115,000 servers deployed in over 973 data center locations in 102 countries. Using these CDN traces, weather data from over 650 locations around the world, and energy price information we evaluate the ability of OAC to reduce operational and capital expenditures via reductions in energy usage and costs.

- *Benefits of OAC:* We study the potential for deploying OAC at scale in a IDS. We design greedy “weather-aware” load balancing algorithms that direct load to the closest data center where the current weather permits “free” cooling using outside air. Our result shows that even during summer, a global IDS can extract more than 51% reduction in the energy spent for cooling using OAC. During winter when OAC is more plentiful, a 92% reduction in system-wide energy can be had. Further, these savings can be achieved without degrading the performance experienced by users. However, important exceptions remain. We find that a city such as Singapore has small or no potential for OAC throughout the year using current technology, while Tokyo is not conducive to OAC during the summer months. However, with newer (class A4) data center technology, even such cities can use OAC, with energy savings for Tokyo rising from 0% to 84% in August.

4.2 Background

In our work, we use (i) the instantaneous weather outside each of the IDS’s data center locations, and (ii) the recommendations of the American Society of Heating, Refrigeration, and Air-conditioning Engineers (ASHRAE) [35] to determine whether the outside air can be used to cool the data center at any point in time. Table 4.1 specifies ASHRAE’s temperature and humidity ranges for four different classes of data centers, where each class represents the type of server and other IT equipment used in the data center. The lowest class A1 represents the most basic equipment that allows the smallest operating ranges of temperature and humidity and as such represent the widest deployment of data centers today. The highest

class of A4 represents the most advanced equipment that can function at a much large operating ranges of temperature and humidity. Given the wide deployment of IDSs, we conservatively assume that our data centers belong to class A1, but also consider what-if scenarios if data centers of higher classes become commonly prevalent. Note that assuming class A1 places a lower bound on the potential savings from OAC.

Class	Dry-Bulb Temp (° C)	Humidity Range	Max Dew Point (° C)
A1	15 to 32	20% to 80%	17
A2	10 to 35	20% to 80%	21
A3	5 to 40	8% to 85%	24
A4	5 to 45	8% to 90%	24

Table 4.1: ASHRAE’s allowable ranges for dry bulb temperature, relative humidity and the maximum dew point of the air that make it suitable for cooling different classes of data centers [35]. Higher data center classes correspond to newer technology allowing for broader ranges of tolerance.

Although ASHRAE standards do not specify the cooling technology to be used by a data center, the specified ranges enable us to determine the upper limits on *outside* air temperature, humidity and dew point that permits OAC to safely cool a data center of a particular class. To determine whether a data center can employ OAC at any point in time, we use the weather data for that location to determine the dry-bulb temperature, relative humidity, and dew point. Following the methodology presented in the GreenGrid consortium whitepaper [35], if the outside air is below the ASHRAE range, it can be rectified by mixing the outside air with the return air that is warmer. Thus, it suffices to compare the measured dry-bulb temperature, relative humidity, and dew point of the outside air with the upper limits of the allowable ranges in Table 4.1 to ascertain OAC feasibility.

Energy Efficiency Metrics: We consider two aspects of efficiency in the context of cooling IDSs: *energy usage* and *energy cost*. Reducing the energy usage reduces carbon emissions, and also reduces energy cost, but not necessarily vice versa. For instance, OAC reduces both energy usage and energy cost. (i) capital expenditure (CAPEX) of cooling

equipment to be installed at a data center, and (ii) operational expenditure (OPEX) of running the cooling system. OAC has the potential to reduce both CAPEX and OPEX of an IDS.

4.3 A Greedy Algorithm for Exploiting OAC

To integrate OAC into an IDS’s architecture, its global load balancer must be made “weather-aware”. The load balancer of an IDS assigns each user request to a “nearby” data center to optimize user-perceived performance. To evaluate the benefit of OAC, we propose a simple greedy algorithm that modifies the load assignments made by the (non-weather-aware) load balancer as reflected in our Akamai load traces by moving user load from data centers that have no OAC to nearby data centers that do, subject to performance constraints. Our greedy algorithm does the following for each of the IDS’s data centers at each time step: if the weather conditions at a data center location permits OAC, then user load mapped to that location is unchanged; however, if the weather conditions at a data center location do not permit OAC, the load balancer attempts to greedily re-assign the load destined for that location to other nearby data centers with spare server capacity where OAC may be available. The premise is that weather patterns exhibit sufficient regional variations so that OAC may be possible at a location even when it is not be feasible at another nearby location. We exploit these geographic variations by searching for alternate “nearby” locations where OAC is still feasible. The pseudocode for this greedy heuristic algorithm is detailed in Algorithm 3.

The primary performance impact to the user from the remapping is that a user may get mapped to a data center that is “farther” away, increasing response times. We can limit how far a user can be remapped by stipulating that our algorithm can only remap load to data centers within a radius r kms of the data center to where it was originally mapped. Specifically, the greedy algorithm reassigns the load of each data center without OAC to alternate data centers with OAC that have spare capacity to accommodate all or part of the load and are within radius r . The alternate data centers are examined in the increasing

Algorithm 3 Pseudocode for Greedy Algorithm for OAC

```
function GREEDYOAC()  
   $time \leftarrow [1, 2, \dots, n]$  ▷ time periods  
   $datacenters \leftarrow [1, 2, \dots, m]$  ▷ data centers  
   $cap \leftarrow [c_1, c_2, \dots, c_m]$  ▷ capacity of data centers  
   $load \leftarrow [l_{11}, l_{12}, \dots, l_{mn}]$  ▷ load for data centers for each time period  
   $sortedpeers_i \leftarrow [p_{i1}, p_{i2}, \dots, p_{ix}]$  ▷ set of peers for each dc i sorted in desc order  
   $oacstatus \leftarrow [s_{i1}, s_{i2}, \dots, s_{in}]$  ▷ oac status for each dc i for each time slot  
   $loadmoved \leftarrow [\delta_{111}, \delta_{112}, \dots, \delta_{mmm}]$  ▷ load moved from dc i to dc j in time t  
  for  $t$  in  $time$  do ▷ for each time slot  
    for  $d$  in  $datacenters$  do ▷ for each data center  
      if  $s_{dt} = 'n'$  then ▷ if oac is not available  
        while  $l_{dt} > 0$  do ▷ while there is still load to move  
          for  $p$  in  $[p_{d1}, p_{d2}, \dots, p_{dx}]$  do ▷ for each peer  
            if  $s_{pt} = 'y'$  and  $c_p - l_{tp} > 0$  then ▷ if oac is available at peer and  
peer has excess capacity  
               $\delta_{dpt} = \min(l_{dt}, c_p - l_{tp})$  ▷ determine load moved based on  
capacity  
               $l_{tp} \leftarrow l_{tp} + \delta_{dpt}$  ▷ adjust loads  
               $l_{dt} \leftarrow l_{dt} - \delta_{dpt}$   
  return  $loadmoved$ 
```

order of distance and any load left unassigned by this process is not remapped and must be cooled in its original data center using traditional HVAC chillers. The radius r represents a tradeoff between network performance and energy savings. The greater the r , the greater the user-perceived response times, but greater are the chances that there will be sufficient geographic weather variations such that OAC is possible at these alternate locations. In general, significant savings are possible with *no performance degradation at all* (i.e., for $r = 0$). Even for moderate values of r (e.g., $r \leq 1000km$), we expect the vast majority of the load to be served locally, while moving the residual load only by a small distance, limiting the potential for performance degradation (cf. Figure 4.6).

4.4 Experimental Methodology

To derive the potential for using OAC in an IDS, we performed trace-driven simulations using a combination of IDS workloads and weather data. We used extensive load data from

Duration	1 month
Resolution	5 minute
Data centers	973 dc locations in 102 countries
No. of servers	115,246

Table 4.2: Load data from Akamai CDN

Duration	12 months
No. of weather stations	13,497
Mapped stations	651
Resolution	1 hour

Table 4.3: NOAA weather data.

across Akamai’s CDN for the period of one month. The trace includes load information from 115,246 servers deployed in 973 data center locations in 102 countries around the world (see Table 4.2). The dataset includes the load, requests served, and bytes served by each server every five minutes over the month-long trace. Further, the trace has detailed information about every data center including the number of deployed servers, total server capacity, and the location of the data center including its latitude, longitude, city, state, and country.

Our experimental evaluation also employs global weather traces provided by the National Oceanic and Atmospheric Administration (NOAA) for the year 2012. The dataset contains year-long weather data from 13,497 weather stations across the globe that record a large number of metrics including the hourly dry-bulb temperature and dew point. Since the exact location of each weather station and data center are known, we can compute the weather station that is closest to each CDN data center and use its weather data to represent the ambient weather conditions at that data center. Given the extensive network of NOAA weather stations, we were able to find a nearby weather station within 10km for the majority of data centers, including all of the “large” data centers near major population centers. We found a weather station within 40km for most of the remaining locations. The matching process yielded 651 weather stations that were mapped onto the 973 data centers (major cities have multiple data centers mapped to the same “nearby” weather station). The weather data was used to determine if the outside air at each data center was suitable for cooling at that time.

To compute the cooling energy required by the CDN, we first compute the server energy consumed (and dissipated) for each data center of the CDN for each 5-minute window

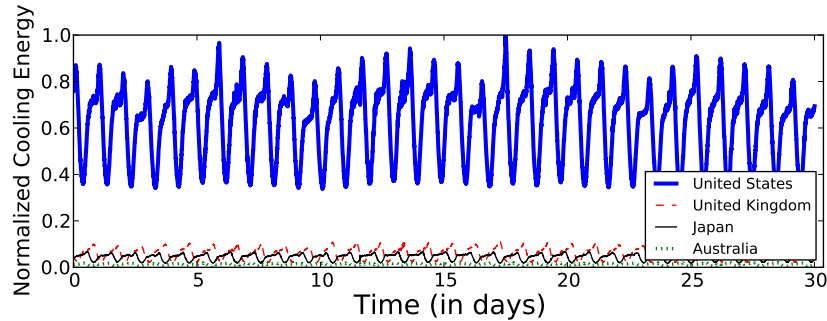


Figure 4.1: Normalized cooling energy required by Akamai’s CDN in the US, UK, Japan and Australia. Notice the diurnal variation as cooling energy is proportional to the load induced by users accessing content from those locations.

using the load and server information in the traces and the server and cluster energy model presented in Chapter 2. Cooling energy is proportional to the server energy, where the proportionality factor is related to the PUE. Figure 4.1 shows the cooling energy required by Akamai’s CDN as computed from the traces for four major countries.

We make two simplifying assumptions in our analysis. We had load data every five minutes but weather data once an hour. We assumed that the weather parameters do not significantly change during the hour. Further, we had weather data for a whole year but comprehensive CDN load data only for a month. We assumed that the measured monthly CDN load pattern repeats through the year.

Our evaluation uses geographic distance as a proxy for latency and response times. This is because our load traces only include client locations and mask client IP addresses for privacy, allowing us to compute geographic distance but not network distance. Prior work has shown that network latency increases with increasing geographic distance, and so distance is a coarse measure of latency (cf. Table 1 of [53], or, Figure 4 of [37] that posits a marginal increase of 1 msec of network latency for every 50km of distance, or [57] that uses distance as a proxy for latency in a similar context).

4.5 Empirical Results

We evaluate the potential for OAC using our greedy algorithm outlined above on our IDS load and weather traces for a full year. In our simulations, we assume that each data center belongs to the most conservative ASHRAE A1 class.

4.5.1 Reduction in chiller capacity

We examine whether OAC can yield CAPEX savings for an IDS. Intuitively, if OAC reduces the worst-case peak demand on HVAC chillers, either by absorbing a portion of the peak demand locally using OAC or by redirecting a portion of the peak load to other nearby data centers that can be open air cooled, then the IDS can deploy lower capacity (and less expensive) chillers to cool the reduced peak load. However, it is not evident *a priori* whether OAC can reduce the worst-case peak demand on chillers, e.g. the worst-case peak load could occur on hot summer days where OAC is infeasible. Figure 4.2 depicts the average capital cost (CAPEX) savings across all global IDS locations due to a reduction in chiller capacity. The figure shows that for A1 class data centers, OAC yields only a 7.5% savings when $r = 0km$, implying that peak load does coincide with hot or humid days when OAC cannot be used. Further, allowing the load to be redirected to locations within a 1000km radius yields 25% CAPEX savings. The CAPEX savings are significantly higher for the newer A4 class data centers with a mean reduction of 68.6% in cooling capex with $r = 0km$ to as much as 89.5% capex reduction when $r = 1000km$.

4.5.2 Reduction in energy usage

Global Savings: The energy savings can be computed by comparing the energy used with OAC to the energy used to cool the original load entirely with chillers without OAC. Figure 4.3(a) depicts the average percentage energy savings obtained across the entire CDN for different months of the year and for different values of distance r . The savings from OAC is generally higher during the cooler winter, early spring and late fall months of the northern

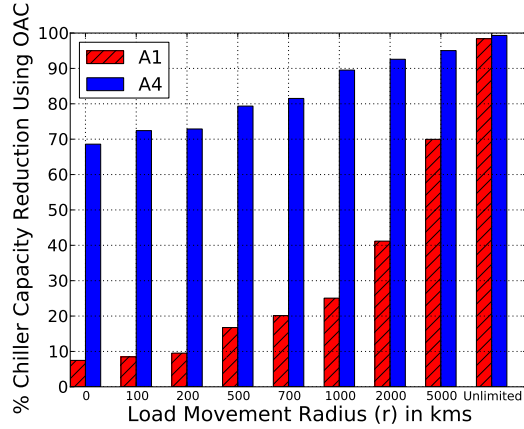


Figure 4.2: Savings in capital costs of chillers with OAC.

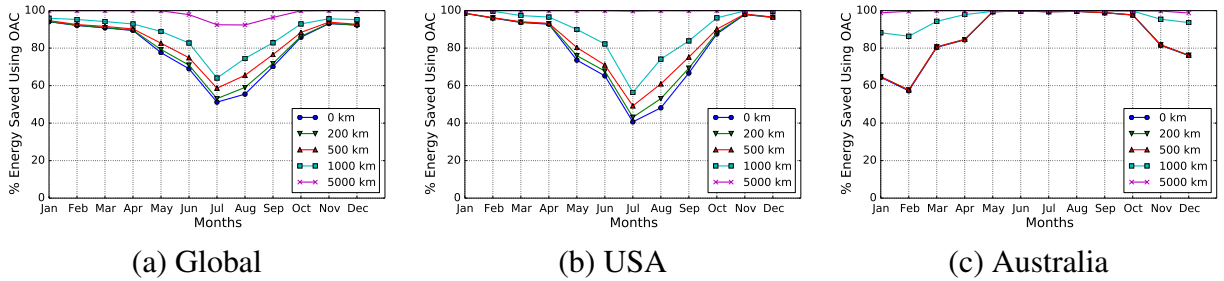


Figure 4.3: Energy savings for the entire global IDS and for major countries in each of the two hemispheres.

hemisphere, with lower savings during the warmer summer months (May to September). Note that our analysis includes savings from data centers in both the northern and southern hemispheres. However Internet traffic from North America, Europe and Asia dominate the global Internet traffic, hence the seasonal benefits from the northern hemisphere dominate the global trends. Overall, our result shows that even during summer, a global IDS can extract significant cooling energy reduction of more than 51% even during summer *with no performance impact* ($r = 0$) and the savings due to OAC increase to over 92% during winter months; the savings increase as the performance constraints are relaxed by permitting $r = 1000km$ yielding an additional 13% savings during the warmest month of July. For $r = 5000km$ which allows for trans-continental load redirection, the savings increase to nearly 92% throughout the year, including summers.

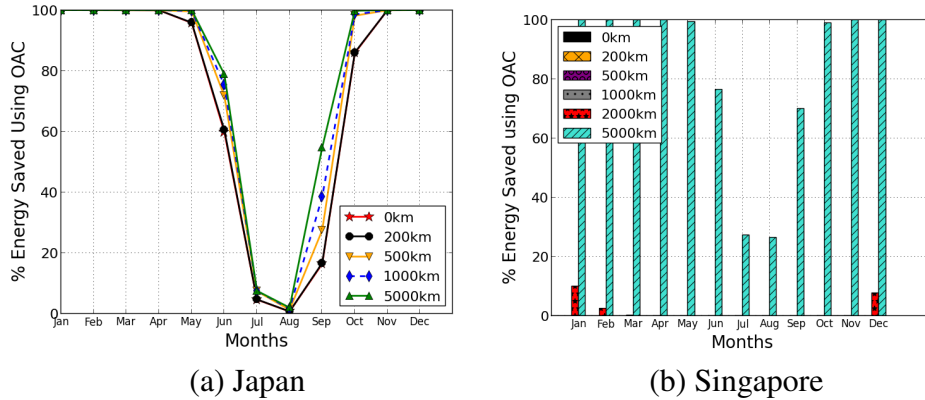


Figure 4.4: Regional and seasonal variations in OAC savings in Japan and Singapore.

Regional and Seasonal Variations in Savings: Figure 4.3(b) and (c) depict the energy savings seen in two major countries, USA and Australia, in the northern and southern hemispheres, respectively. Energy savings in USA broadly follow the global trends, indicating that USA not only contributes a significant portion of the global traffic, but also has its seasons aligned with the dominant northern hemisphere. Further, USA being a large country in terms of geographic area, exhibits significant regional variations. Fig 4.3(b) shows high energy savings of 96% in winter months, it indicates that most cities, regardless of location, see uniformly high energy savings. In the summer, however, there are considerable differences: southern cities such as LA see low OAC savings (for $r = 0$), while northern cities such as Seattle see higher than average OAC savings. Australia (in Fig 4.3(c)) sees similar differences between summer and winter, with OAC savings of 64% in the summer month of January for $r = 0$ and nearly 100% savings in the winter months of May to September. Further, allowing the load re-direction to a data center within a 1000km radius increases the summer savings to above 85.6%.

Since Asia has less temperate climate than North America or Australia, our results show significant regional and seasonal differences in the savings obtained from OAC. Japan (cf. Figure 4.4(a)) has the most significant seasonal variations in OAC benefits—with nearly 100% energy savings from employing OAC during the winter months to a zero savings in the

summer month of August for the no load redirection scenario of $r = 0$. While Japan exhibits the extreme seasonal variations in OAC benefits, Singapore (cf. Figure 4.4(b)) sees the worst year-round benefits. While Singapore is itself a small country, it is a key regional “hub” with significant traffic. Since Singapore is located near the equator, it has warm and humid weather throughout the year with nearly no seasons. Consequently OAC is not possible in Singapore during any month of the year, yielding zero savings. Even allowing Singapore traffic to be sent to data centers within a 1000km radius yields no benefits.

4.5.3 Impact of Newer Data Center Technologies:

Thus far, we assumed that all IDS data centers belong to the most conservative *A1* class in terms of server and cooling equipment. However commodity servers built in recent years are engineered to withstand higher temperatures without impacting reliability. Further, the latest cooling equipment can deal with a larger range of humidity scenarios. Consequently, we repeat the previous analysis by assuming all data centers are built for ASHRAE’s most aggressive *A4* class, which permits the inside temperatures in the data center to be maintained as high as 45°C with relative humidity of 90 (cf. Table 4.1). Our experiment sheds light on the additional benefits from having *A4* class data center, since OAC now becomes feasible even in warmer or more humid climates. With *A4* class, we observe 95% energy savings from OAC year-round for $r = 0km$, with a slight decrease in the summer. With $r = 1000km$, the savings rise to 98% even in the summer. In addition to *A4* class of data centers, we also perform the experiment with the intermediate *A2* type data centers. As we can see in Figure 4.5, globally we see higher than 70% savings for 0kms year round. If we allow a radius of 1000kms, we see a savings close to 90% with a slight dip in the summer.

4.5.4 Network latency impact

Figure 4.6 shows the impact on performance (i.e., latency increase) due to OAC-driven load movements is likely to be small even when we allow our algorithm to move load to data centers that are up to 1000km away. This is because over 90% of the load is served

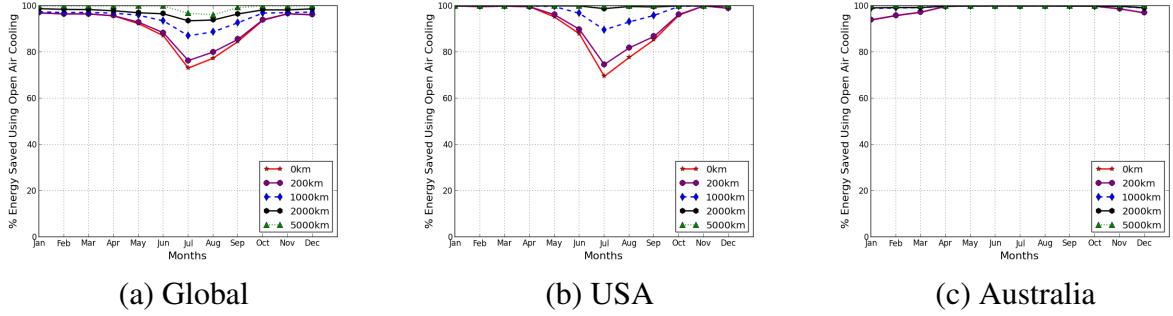


Figure 4.5: Energy savings for the entire global IDS and for major countries in each of the two hemispheres for A2 data centers.

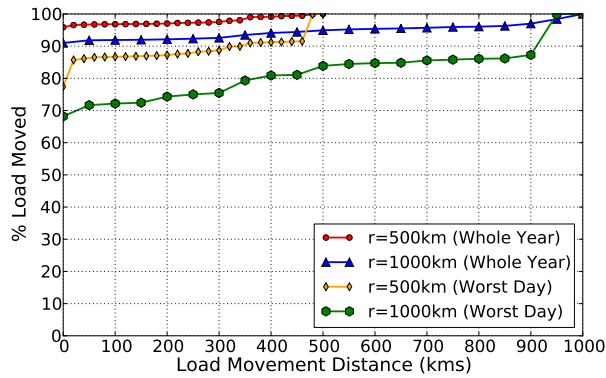


Figure 4.6: Average distance the load is moved by our algorithm for the whole year and on the worst day for $r = 500$ and 1000 .

locally due to OAC on an average day; even on the worst day of the year, over 68% of the load is not moved at all. On an average, 92.6% (resp. 97.5%) of the user load gets served by a data center within 300km for $r = 1000km$ (resp. $r = 500km$). Even on the worst day of the year that requires the most load movement, 75.5% (resp., 88.7%) of the load is served by a data center within 300km for $r = 1000km$ (resp., $r = 500km$). These results indicate that only a few users see a modest increase in latency due to OAC while most see no impact.

4.6 Implications for IDS Design

We showed that IDSs can significantly reduce brown energy consumption for A1 type data centers by leveraging OAC availability at diverse geographical locations using our load

shifting algorithm. We also showed that there is not a large increase in latency for IDS users. Given operating ranges of temperature and humidity are even more relaxed for A2 through A4 type data centers, they will see higher savings in energy reduction and capital expenditure. Therefore, IDSs should be designed to incorporate OAC and OAC-based load shifting to the extent possible.

4.7 Related Work

Data centers and IDSs consume a significant amount of energy and techniques to reduce the energy consumption have been studied extensively. Much of this effort has focused on reducing the power consumption of server clusters through advanced cluster-wide power management techniques [17, 43]. In the IDS context in particular, techniques such as server- and cluster shutdown have been proposed to make server clusters more energy proportional to IDS traffic [49]. Moving load across data centers of an IDS to exploit variation in energy market prices [57] and for increasing the use of renewables [47] has been studied. However, we explore load movement for evaluating the potential for OAC using extensive IDS load and global weather traces. Separately, the use of renewable energy to power and cool data center servers [45] and techniques to minimize server carbon footprint [27] have also been studied. In the context of reducing the cooling energy, thermal engineering techniques have been studied to optimize temperature and air flow through server racks or perform temperature-aware scheduling of workloads on “cool” racks [21]. However, the use of new cooling technologies in data centers has only recently begun to gain attention [11, 45]. In the context of OAC, recent ground-breaking work has focused either on the systems aspect of incorporating OAC into a modular data center [22] or on provisioning [48] and temperature management [31] within a single data center. Work has also shown that significant savings in energy can be achieved within a data center by the use of renewable cooling technologies [70]. Companies such as Facebook have begun to employ open air cooling in their data centers in recent years [68].

4.8 Conclusions

In this chapter, we studied the potential benefits of using OAC to reduce the energy usage as well as the operational and capital costs incurred by an IDS for cooling its servers. We presented algorithms to incorporate OAC into the IDS architecture and empirically evaluated its efficacy using extensive traces from Akamai's global CDN and global weather data from NOAA. We showed that, by using OAC, a global IDS can extract a 51% cooling energy reduction during summers and a 92% reduction in the winter. Further given ASHRAE's new operating temperature limits and the ability of IDSs to lend themselves to load shifting across data centers, we can significantly reduce, and in some locations, nearly eliminate cooling costs. Overall, we show that OAC holds great promise for the future sustainable IDS design.

CHAPTER 5

COMBINING SOLAR ENERGY AND OPEN AIR COOLING FOR GREENING INTERNET-SCALE DISTRIBUTED SYSTEMS

In the previous chapters, we considered renewable power and renewable cooling separately to green IDSs. Motivated by the contrasting nature of solar energy and OAC, we now study the benefits of combining these two renewable technologies to help us green IDSs. We note that solar energy is more abundant in sunny locations and during day-time. In contrast, OAC is available when the weather outside is cold and dry enough. Therefore, OAC is available in colder locations and during night-time. We evaluate if the contrasting nature of these two technologies yields complementary benefits. Given renewables are intermittent in general, and the renewables we have chosen to study are complementary in time and space, we use batteries and load shifting for smoothing the supply of green energy. We study the greening potential of combining these two technologies against two yardsticks: reduction in brown energy and cost effectiveness. To realistically evaluate the greening potential, we use an extensive real-world load trace from Akamai, one of the leading CDN providers in the world [53].

5.1 Contributions

To the best of our knowledge, our solution is novel as it synthesizes two renewable technologies, solar energy and OAC, and evaluates their greening potential in the context of an IDS, with large-scale real-world load traces. Specifically, our contributions include:

- *Synthesizing solar energy and OAC as contrasting and complementary technologies:* Motivated by the contrasting and complementary nature of solar energy and OAC, we use a

simple greedy algorithm that enables us to use solar energy and OAC efficiently. A *net-zero year* (nzy) data center produces as much energy from renewables in a year as it needs to entirely offset its brown energy consumption in that year. Just by introducing OAC alone to the mix of half the number of panels it takes to be net-zero year, we show that we can go from 34% reduction to about 54.9% brown energy reduction. With panels needed to be net-zero year, we can go from 41.5% to about 59.4% savings. We see even higher savings by employing both batteries and load movement. We incorporate several key parameters that can be used to model trade-offs while evaluating energy efficiency. Some of these parameters include radius of load movement, battery capacity, number of solar panels installed, battery cost and lifetime, solar panel cost and lifetime, and energy prices.

- *Evaluation using an extensive real-world trace:* We evaluate the greening potential of solar energy and OAC using extensive load traces from Akamai [53]. The dataset used consists of information on from 724 global data center locations including 100,592 servers deployed all over the world. We also use year-long weather data for OAC from over 650 locations. In addition, we use a year's worth of PVWatts solar data. Using this data, we simulate our solution for a whole year, parallelizing our runs by week to reduce the time of running. We then evaluate our solution against several metrics measuring total brown energy reduction, peak reduction, cost savings and a break-even analysis. We vary battery capacity as a function of the average day's load in a data center.

- *Brown energy reduction evaluation:* We evaluated how well the mix of solar energy and OAC reduces brown energy consumption. Energy companies often charge their customers for both the energy consumed and the peak energy drawn. As part of this analysis, we studied two metrics: 1) total brown energy reduction and 2) peak energy reduction. For brown energy reduction, we studied how our results vary with addition of OAC to solar energy, with the addition of load movement, and also with the addition of batteries.

Allowing a radius of 5000kms with the combination of solar energy and OAC, we can increase our savings to 60.3% or panels0.5 and to about 65% with net-zero year panels.

Our results show that with a battery capacity of half the average day's load at each data center, we can significantly increase the reduction in brown energy to over 73% for panels 0.5 and over 89% with net-zero year panels, without moving any load. For percentage peak reduction, we see a reduction between 10% and up to 40% depending upon the number of panels installed, the battery capacity and radius of load movement. Fixing the radius of load movement to 1000kms, and varying battery capacity and panels as shown above, we can achieve a reduction of about 11% in the worst case to about 26% with greater battery capacity and larger number of panels.

- *Results on increasing green energy utilization:* We evaluated how much green energy we can utilize under different conditions. Without any load movement and with 0.5 times the panels we need to be net-zero year, if we employ a battery about 0.5 of the average day's load, we can increase green energy utilization from about 72% to over 95%.

- *Amortized cost analysis:* We evaluated the cost saving potential of our solution given investment in different combinations of battery capacities and number of panels. We calculated yearly cost savings based on yearly savings in brown energy consumption costs and yearly amortized expenditure for batteries and panels. We find significant cost savings for moderate and high energy prices, ranging from 9.9% all the way to 60.3% based on different parameter values. Even for low price for energy, if we do not use batteries and have 0.5nzy panels, we see cost savings from 22% to 41%. However, with 0.5avgdayload batteries and 0.5nzy panels, savings drop to between 3% to about 8.4%, and for other combinations of panels and batteries we incur a loss in the case of low price of energy. With the prices of batteries and solar panels on the decline, we believe the results for lower energy prices should also improve in the future.

- *Break-even analysis:* With a higher price of energy, for half the panels it takes to be nzy, we see break-even periods as low as 6 years. For a moderate and low energy prices, we can achieve break-even periods of 8.9 years and between 14.9 years respectively. Again,

with the cost of solar panels and batteries declining, these numbers should improve in the future.

- *Cost Analysis based on future projections:* Given the price of solar panels and batteries is falling, and the price of energy over the long run is increasing, we evaluated our solution using projected prices of batteries, panels, and energy. We found dramatic increases in brown energy reduction and break-even periods even for the projected lower end price of energy. Even for the low price of energy, for which we incurred a loss in certain cases with current prices, we see cost savings of 23.9% to 55.9%.

5.2 Background

Geographical Variations in Solar Energy and OAC Availability: We see variations in solar output and OAC based on factors like temperature, season, time of day, northern or southern hemisphere location, climate, weather conditions [33] [34]. Therefore, using renewables efficiently involves handling the variations in and availability of renewable output. In this paper, we use a combination of load movement and battery storage to mitigate the problem of intermittent availability of solar energy and OAC. Given the geographical diversity of data center locations and replicated content and services, we use load shifting to take advantage of renewables. We vary radii of load movement to control latency. To enable us to store excess solar energy, we assume that batteries are available at all data center locations. We vary battery capacity installed at a data center location as a function of the average day's load for that data center. We also consider the case where net metering is available at all data centers and calculate energy savings with net metering.

Metrics for evaluating proposed solution: To evaluate the combined greening potential of solar energy and OAC, we measure reductions in both *energy consumption* and *cost*. We use reduction in total brown energy consumption, green energy utilization, and reduction in peak energy drawn from the grid to determine how effective the combination of solar

Variable and Value	Notation
battery capacity = x *(avg day's load)	bcap x
num solar panels = x *(net-zero year number of panels)	panels x or xnzy
radius of load movement = x kms	$r=x$

Table 5.1: Parameters values and related notation used to refer to them in the paper energy and OAC is in greening IDSs. We use amortized cost savings and a break-even analysis to evaluate how effective the algorithm is with respect to cost.

Parameter Values and Related Notation: In this paper, we study our algorithm by varying parameters like battery capacity and number of solar panels. We vary battery capacity installed at a data center as a function of the average day's load for that data center. We consider three different fractions: 0, 0.5*(average day's load), and 1*(average day load). We vary the number of solar panels as a function of the net-zero number of panels for a data center. We consider two fractions: 0.5*(net-zero year number of panels), and 1*(net-zero year number of panels). In addition to these, we also vary the radius of load movement and use a notation $r=x$ to mean that a maximum radius of load movement of x kms was used in our simulation. It is cumbersome to refer these cases using their full descriptive text for battery capacity and panels as listed above. Therefore, we use a shorter notation and list the mapping of the full text to its notation in Table 5.1. For example, to refer to a case in which we employ a battery capacity of 0.5*(average day's load) and install 0.5*(net-zero year number of panels), in our plots and empirical results we use a notation *bcap0.5 and panels0.5 (or 0.5nzy)*.

Problem Statement: As explained earlier, IDSs consume a significant amount of energy. The bulk of the energy consumed by data centers consists of energy used to power servers and to cool them [56]. One way IDSs can be made greener is by replacing brown energy consumption by energy generated from renewable sources. Solar energy is correlated with sunny weather and day-time. In contrast, OAC is more abundant in colder weather and night-time. In this paper, we study the potential of using two *contrasting* and *complementary* sources of renewable energy (namely solar energy and OAC) in their ability to reduce brown

energy consumption in IDSs in a cost effective fashion. Given the intermittent nature of renewable energy, in general, and the complementary nature of these two specific sources, we use batteries and load movement as facilitators for smoothing supply of green energy. Specifically, in this paper we try to study two aspects:

- *The potential for replacing brown energy with a combination of solar energy and OAC in IDSs.*
- *The cost effectiveness of combining these two contrasting sources of renewable energy in our IDS setting.*

5.3 Energy-Aware Load Scheduling Algorithm

We describe our greedy heuristic algorithm in the following paragraphs. We assume that we have the ability to cool load using OAC as long as the weather conditions outside permit us to do so. We also assume we have the on-site solar panels at each data center location. Further, we assume that we have batteries available locally to store excess solar energy. Finally, we assume we can leverage redundancy and data replication in IDSs by moving load to locations where there is more renewable energy available.

Our algorithm works as follows. If OAC is available, we use that for cooling data centers. If solar energy is being generated by locally installed solar panels, we use that to meet local energy demand, including cooling energy if OAC is not available. For remaining server and cooling load, we use locally installed batteries. If any load is left over, we try to shift it to other locations with surplus green energy, constrained by a maximum radius of load movement. We do load shifting in two iterations. In the first iteration, we move load to locations that have both surplus solar energy and OAC. In the second iteration, we move load to locations that have surplus solar energy and no OAC. This allows us to use solar energy from data centers that did not get selected in the first iteration. For both iterations, load shifting is constrained to remain within a maximum radius of load movement to control

latency. Finally, for any remaining load, we draw energy from the grid. We store any unused solar energy in batteries for future use. The pseudo-code for the algorithm is listed in Algorithm 4.

Algorithm 4 Greedy Algorithm Pseudocode

```

1: function GREENHEURISTIC( )
2:    $dcs \leftarrow [1, 2, \dots, m]$  ▷ datacenters
3:    $sortedpeers \leftarrow [p_1, p_2, \dots, p_m]$  ▷ sorted list of dc peer dcs in increasing order of dist
4:    $time \leftarrow [1, 2, \dots, n]$  ▷ time periods
5:    $r = \text{max radius of load movement}$ 
6:    $b \leftarrow [b_1, b_2, \dots, b_m]$  ▷ battery charge
7:   for  $i$  in  $time$  do
8:      $sload \leftarrow [l_{11}, l_{12}, \dots, l_{mn}]$  ▷ server load for time period
9:      $cload \leftarrow [c_{11}, c_{12}, \dots, c_{mn}]$  ▷ cooling load for time period
10:     $oac \leftarrow [o_{11}, o_{12}, \dots, o_{mn}]$  ▷ oac available y/n?
11:     $solarenergy \leftarrow [s_{11}, s_{12}, \dots, s_{mn}]$  ▷ local solar energy
12:     $surpluslist \leftarrow []$  ▷ to store dcs with surplus solar energy
13:     $deficitlist \leftarrow []$  ▷ to store dcs using brown energy
14:    for  $j$  in  $dcs$  do
15:      if  $o_{ij} = y$  then
16:         $c_{ij} \leftarrow 0$  ▷ if there is OAC, cooling load is zero
17:         $excessSolar_{ij} \leftarrow s_{ij} + b_j - (l_{ij} + c_{ij})$  ▷ determine excess solar
18:        if  $l_{ij} + c_{ij} > s_{ij}$  then
19:           $b_j \leftarrow b_j - (l_{ij} + c_{ij} - s_{ij})$  ▷ use battery if solar energy falls short
20:        if  $excessSolar_{ij} > 0$  then
21:           $surpluslist \leftarrow surpluslist \cup [j]$  ▷ add dc to surplus list
22:        else if  $excessSolar_{ij} < 0$  then
23:           $deficitlist \leftarrow deficitlist \cup [j]$  ▷ add dc to deficit list
24:        for  $j \in deficitlist$  do ▷ first iteration
25:          for  $p \in sortedpeers$  do
26:            if  $p \in surpluslist \wedge o_{ip} = y \wedge dist(j, p) \leq r$  then
27:              move load to p and adjust variable values
28:          for  $j$  in  $deficitlist$  do ▷ second iteration
29:            for  $p \in sortedpeers$  do
30:              if  $p \in surpluslist \wedge o_{ip} = n \wedge dist(j, p) \leq r$  then
31:                move load to p and adjust variable values

```

Parameter	Value
Loss %	14
System Capacity	0.275 kW
Module Type	Standard
Timeframe	Hourly
Azimuth	180 deg for northern hemisphere and 0 for southern
Tilt	Absolute value of latitude
Dataset	'TMY2' for US Locations and 'Intl' for others

Table 5.2: Parameters for PVWatts Data

5.4 Experimental Methodology

We performed our experiments on a month-long Akamai trace. This extensive trace has a granularity of 5 minutes and consists of information on 100,592 servers in 724 global data center locations from around the world. The data set consists of information for fields like load, requests, bytes, number of servers, server capacity, latitude, longitude, city, state, and country.

Our solar data set was acquired from the PVWatts [52] website. It consists of a year-long dataset for solar energy generation at a granularity of one hour. We assume that the power rating of a solar panel ranges from 200 watts to 350 watts [24] and take an average value of 275 watts as the power rating per panel. We list values of parameters used for PVWatts solar data in Table 5.2. For any other required parameters, we used the default values listed in the PVWatts version 5 manual [20].

For determining OAC availability we used a year-long weather dataset for the year 2012 from the National Oceanic and Atmospheric Administration (NOAA). This global dataset contains several metrics, including hourly dry-bulb temperature and dew point. Given that the location of our data centers, we mapped which weather station was closest and used its weather data as being representative of the weather at the data center location. Given the NOAA has a vast network of weather stations, we could map most of our data centers to weather stations within 10kms. For most of the remaining data centers, we could map a weather station within 40kms.

Weather data used for OAC and solar data had a granularity of one hour. However, the load trace has a granularity of 5 minutes. We therefore assumed that the weather and solar output do not change much during the hour, and use the hour's value for each of the 5-minute timeslots that fall within the hour. Additionally, our weather data and solar energy data was year-long, however, the Akamai load trace was month-long. To simplify, we assumed that the load trace pattern repeats throughout the year. However, our algorithm does not fundamentally depend upon or exploit the fact that the load pattern repeats throughout the year. Therefore, it would also be applicable to a yearly load trace in which the load pattern is different for each month.

We analyzed our metrics by varying several parameters. For a given data center, we varied battery capacity as a function of the average day's load, and considered battery capacities of zero, half of the average day's load, and a full average day's load. For each data center, we determined the number of solar panels we need to be net-zero year i.e. the number of panels needed to produce enough solar energy to cover the total energy needs of the data center for a year. For our experiments, we varied the number of panels from half of the net-zero year number of panels to a full net-zero year number of panels. Given the size of our datasets, running our algorithm sequentially would have been computationally expensive. Therefore, we parallelized our algorithm by week and in order to do a worst case analysis, we assumed a starting battery charge of zero at the beginning of each week.

5.5 Empirical Results

We evaluated the greening potential of solar energy and OAC in the context of both brown energy reduction and cost effectiveness. We analyzed several metrics, namely brown energy reduction, green energy utilization, peak reduction, cost savings, and break-even points. We describe our findings related to these metrics in the paragraphs below.

5.5.1 Brown Energy Reduction

Brown energy reduction is calculated by taking the average of percentage reduction in brown energy across all the data centers of the IDS for the year. Our results show the following:

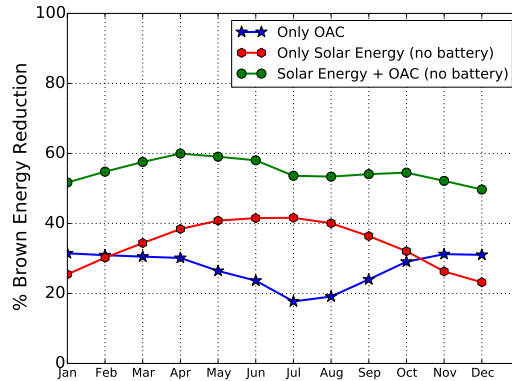


Figure 5.1: Plot shows how solar energy and OAC combine to yield higher savings across various months of the year for panels0.5 and $r=0$.

- *Combining solar energy and OAC yields significant benefits:* Figure 5.1 shows the brown energy reduction we can achieve with the combination of solar energy and OAC by different months of the year. Solar energy output is higher in the summer months when there is plenty of sunshine. Therefore, we see the reduction in brown energy peak in the summer months when we use solar energy alone. In contrast, OAC is more abundant when the outside weather is cold and dry enough. Therefore savings from OAC are higher in the winter months and dip in the summer months. Combining these two technologies, we can achieve a much higher savings of between 49.7% to about 60% throughout all the months of the year as shown by the green line. Figure 5.4 shows how our yearly average percent savings increase when we combine solar energy with OAC. As seen by comparing the left two bars of Figure 5.4 (a) and (b), just by introducing OAC alone to the mix of 0.5nzy panels, we can go from 34% reduction to about 55% average brown energy reduction. With nzy panels, we can go from 41.5% to about 59.4% savings.

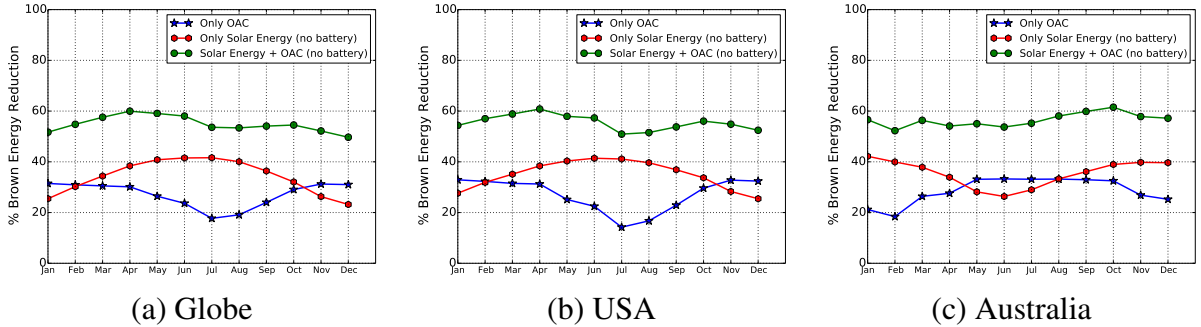


Figure 5.2: Figures show the break-up of brown energy reduction for only solar, only oac, and solar plus oac with bcap0 and panels0.5nzy

- Northern and Southern Hemisphere Differences:* Figures 5.2 and 5.3 show the break-up of savings for different months for the globe, USA and Australia. Figure 5.2 shows results for the case when battery capacity is zero, and Figure 5.3 shows plots for the net metering (or infinite battery) scenario. Firstly we see that in the northern hemisphere (e.g. in USA), the savings from solar energy are pronounced over summer, whereas savings from OAC are pronounced over winter. In the southern hemisphere (e.g. in Australia as seen in Figure 5.2 (c)), this trend reverses. The global results are dominated by USA traffic and show similar trends. In all cases, combining solar energy and OAC (green line in the plots), we see that we can increase and smooth out savings significantly over all months of the year.

- Net metering increases savings significantly:* Corresponding plots of Figures 5.2 and 5.3 show that with net metering we can see a dramatic increase in brown energy reduction for all months of the year. For example, as we can see from the green lines in Figures 5.2 (a) and 5.3 (a) the combined OAC and solar energy savings for the globe increase from an average of about 54% (without net metering) to an average of about 77% for the year (with net metering).

- Load movement leads to more savings:* As seen in Figure 5.4 (a and b), savings increase with increasing r . For $r=5000\text{kms}$, we can increase our average reduction from 54.9% to 60% for panels=0.5nzy and from 59.4% to 65% for nzy panels.

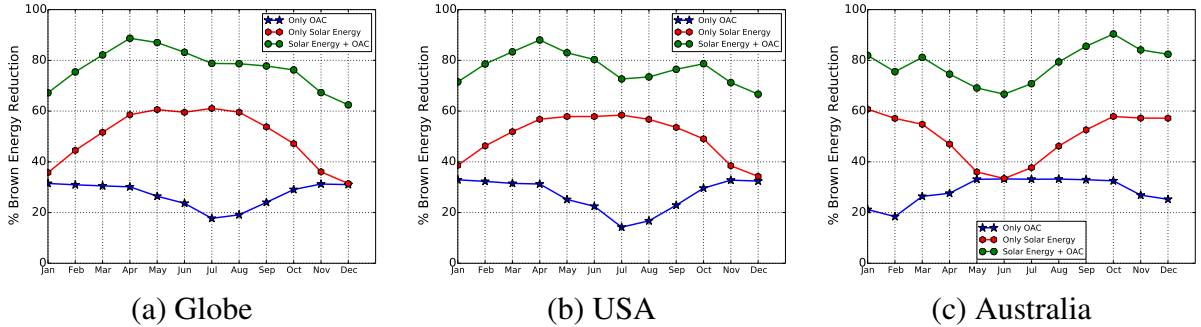


Figure 5.3: Figures show the break-up of brown energy reduction for only solar, only oac, and solar plus oac with net metering and panels0.5nzy

- Batteries help significantly:* As seen by the leftmost bars in Figure 5.4 (c and d), in the absence of batteries, doubling the number of solar panels increases savings from 34% to 41.5% for the solar energy only scenario and from 54.9% to only about 59.4% for the combination for solar energy and OAC. Without batteries, instantaneous solar energy produced is wasted. However, as shown by the bars to the right in Figure 5.4 (c), by employing batteries with bcap0.5, we can significantly increase the reduction in brown energy to over 48% for panels0.5 and over 74.9% for nzy panels with solar energy alone. For the combination of solar and OAC in Figure 5.4 (d), we can increase savings to 73% for 0.5 net-zero year panels and over 89% with net-zero year number of panels.

- Diminishing returns with increase in battery capacity:* Reduction in brown energy increases with larger battery capacity, however, we see diminishing returns. Figure 5.4 (d) shows the jump in savings from 0 battery capacity to 0.5 is dramatic – from 54% to 73% for 0.5nzy panels. However the jump from 0.5 to 1 is not that large – 73.2% to 73.7%. For a larger number of solar panels (shown by the red bars in Figure 5.4 (d)), the same diminishing returns with batteries are observed and we see a jump in reduction from 59% to 89% to 91% as we increase the battery capacity from 0 to 0.5 to 1. This trend is also preserved for the solar energy only scenario as we can see from Figure 5.4 (c).

- Application-specific parameter values:* We can achieve similar gains in brown energy reduction with different sets of parameter values. These parameter values could be chosen

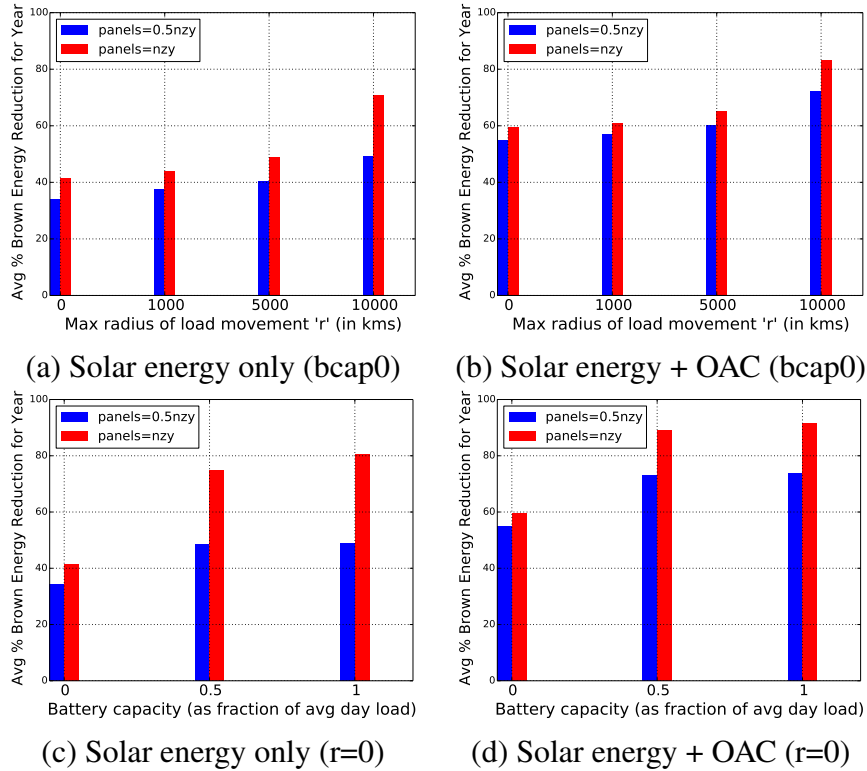


Figure 5.4: We see a significant increase in brown energy reduction as we move from solar energy only (a & c) to solar energy + OAC (b & d). Increasing r (a & b) yields larger savings. Increasing battery capacity (c & d) helps but shows diminishing returns.

based on the specific needs of applications, e.g. we may choose to not move load for latency sensitive applications, whereas for latency tolerant applications, we may choose to move load and save on battery costs. As an example, suppose we would like to achieve approximately 70% reduction in brown energy consumption. We can achieve this in two different ways using different combinations of load movement, battery capacity, and solar panels. The two ways from the above plots are: From Figure 5.4 (b), bcap0 panels0.5 and $r=10,000$ and from Figure 5.4 (d), panels0.5 bcap0.5 with $r=0$. The former scenario is better suited for applications that can tolerate latency, whereas the latter can be employed in case of latency-sensitive applications though with an added expenditure for batteries.

- *Location Based Results:* Trade-offs for specific locations vary significantly depending on the local availability of solar energy and OAC and their interplay. For a place like Anchorage (see lowest blue line corresponding to panels0.5 bcap0 in Figure 5.5(a)), where

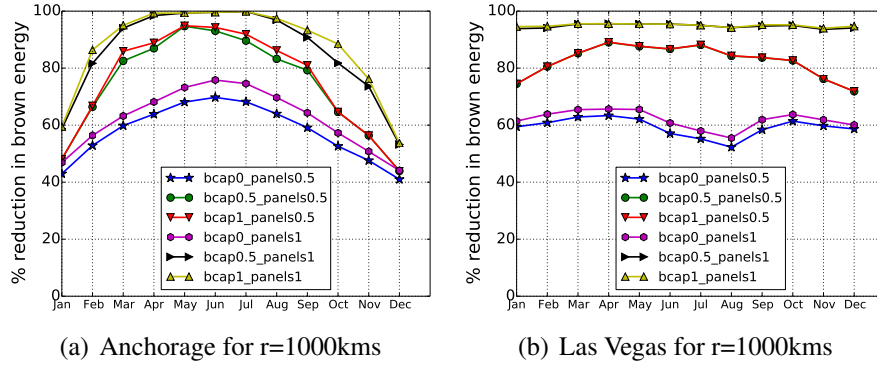


Figure 5.5: Figure showing reduction in brown energy across different months for Anchorage and Las Vegas

OAC is available for most of the year, the shape of the curve depends on the availability of solar energy, which peak in the summer months. However, for a place like Las Vegas (see lowest blue line corresponding to panels0.5 bcap0 in Figure 5.5(b)), where solar energy is available for most of the year, we get a curve that dips in the summer months, when OAC is not as abundant. These shapes change with the addition of load movement and batteries to the mix, as both of those alter the basic assumptions about locational variations of OAC and solar. Also, locations that are mostly high in solar energy output (e.g. Las Vegas which is ranked as the third highest city in the United States based on percentage annual sunshine [50]), have an advantage over locations that are excellent for OAC year round (e.g. Anchorage where the highest average year round temperature is 19 °C and the average dew point is -2 °C [67]). Solar output can be used for meeting both server energy demand, as well as for cooling purposes. However, OAC can only be used for cooling. From the plots, with sufficiently high number of solar panels and battery size, we can nearly see a high reduction in brown energy consumption year round. For Anchorage, however, in the summer months we see a dip in brown energy reduction due to lesser solar energy availability. The curves also show diminishing returns when battery capacity is increased successively from zero, to half of the average day’s load, to a full average day’s load.

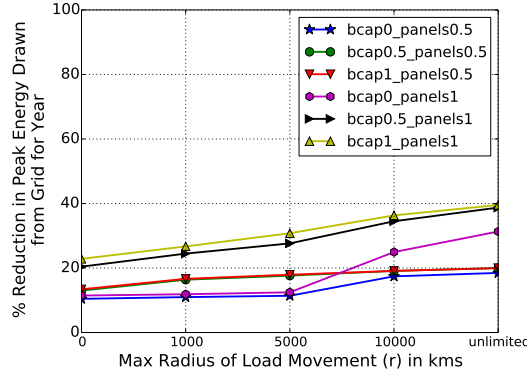


Figure 5.6: Plot showing significant gains in peak reduction. Increasing solar panels, battery capacity and r result in higher reductions.

5.5.2 Peak Reduction

This metric measures the average percentage peak reduction for peak energy drawn from the grid for the year. We first determine the maximum energy drawn for a data center for the year for the original load trace. We then determine the maximum energy drawn for the new load incorporating solar panels, OAC and load movement (for $r > 0$) under the greedy heuristic algorithm. We then calculate the percentage reduction for each data center based on the above values and finally average them. Our results are shown in Figure 5.6.

- *Significant reduction in peak energy:* As shown in Figure 5.6, we can see an overall reduction between 10% and up to 40% depending upon the number of panels installed, the battery capacity and radius of load movement. Fixing the radius of load movement to 1000kms, and varying battery capacity and panels as shown above, we can achieve a reduction of about 11% in the worst case to about 26% with greater battery capacity and larger number of panels. With a larger radius of load movement, we can see significantly higher percentages of reduction. As an example, with a $r=10,000$ kms we can see a decrease of over 35% with bcap1 and nzy panels.

5.5.3 Green Energy Utilization

Green energy utilization measures how much green energy, including energy from solar panels and OAC, is being utilized as a percentage of total green energy available. To

determine green energy utilization we first determine the total green energy being consumed at all data centers for the year and then calculate utilization as a percentage of the total green energy supply. The total green energy supply is the total solar energy produced by the net-zero year number of panels installed at the data center and the amount of OAC available. As a simplifying assumption, we assume that if the outside weather permits, we have as much OAC available as the cooling energy demand at each data center. Figure 5.7 includes results for this metric.

- *Batteries help significantly:* Batteries are important in increasing green energy utilization. Fig 5.7 (a) shows that without any load movement and with 0.5 times the panels we need to be net-zero year, if we employ a battery about 0.5 of the average day's load, we can increase green energy utilization from about 72% to over 95%. With net-zero year panels, we can increase green energy utilization from 47.4% to about 72.95%.

- *Load movement helps in the absence of batteries:* We observe from fig 5.7 that load movement helps over larger values of r without batteries. To control latency, our algorithm gives preference to the utilization of local green energy first, and so with batteries load movement does not help as much. Without batteries, we see a considerable gain in green energy utilization over larger distances. in increasing green energy utilization. Without load movement and without batteries, we see a utilization of about 71.6%. However, with $r=10,000$ kms and without batteries, we can achieve close to about 93% utilization.

- *Diminishing returns with increase in battery capacity:* As fig 5.7a above shows, this metric also shows diminishing returns with increasing battery sizes. Both series level off after their first significant jump when we go from zero battery capacity to a capacity of 0.5 times the average day's load. With fewer panels (0.5 net-zero year), with increasing battery capacity, we see the utilization go up from 72% to about 95% to 95.8%. For net-zero year panels the numbers are 47.4% to 70.97% to 72.95%.

- *Application specific configuration:* With $bcap0$ panels0.5 and $r=10,000$ and panels0.5 $bcap0.5$ with $r=0$, we can achieve more than 95% green energy utilization as shown in

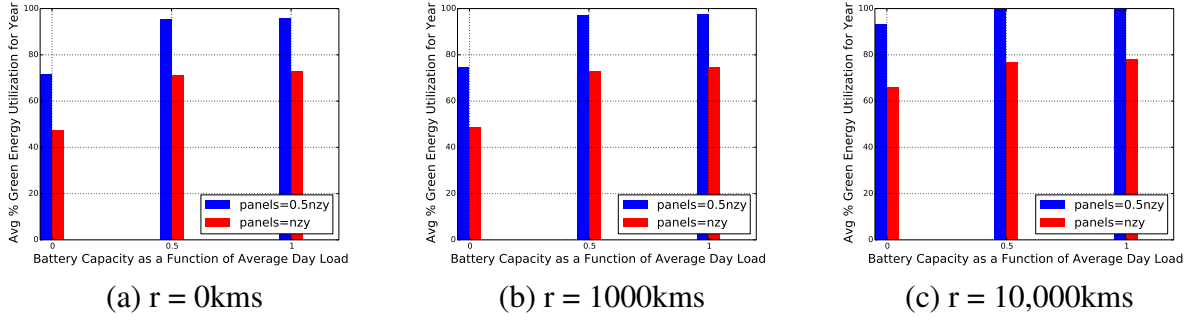


Figure 5.7: Plots show that batteries help with increasing green energy utilization. Load movement also helps in increasing green energy utilization over larger values of r

Resource	Parameter	Value
Battery	Price/kWh lifetime	\$190/kWh 10 yrs
Solar Panels	Price/Wac lifetime	\$2.1/Wac 25 yrs

Table 5.3: Price and lifetime for batteries and solar panels. Cost for commercial solar panels and lithium-ion batteries was used.

Fig 5.7 a and Fig 5.7 c, . The former case may be more suitable for applications that are latency sensitive, where as the latter may be acceptable for applications where latency is not a serious issue.

5.5.4 Cost Analysis

In this section, we evaluate how well the combination of solar energy and OAC performs with respect to cost savings. To this end, we consider the following aspects: 1) Yearly amortized cost savings and 2) Break-even analysis. We describe these in detail in the following paragraphs.

With the battery and solar cost and lifetime parameters [14] [63] [51] [23] listed in Table 5.3, we studied cost savings and break-even periods under three different prices of energy from low, to moderate, to high. The following three scenarios were analyzed:

- **Low Price - 7¢/kWh:** This is closer to the industrial price of electricity in the US [7] and is the lower end price for our analysis.

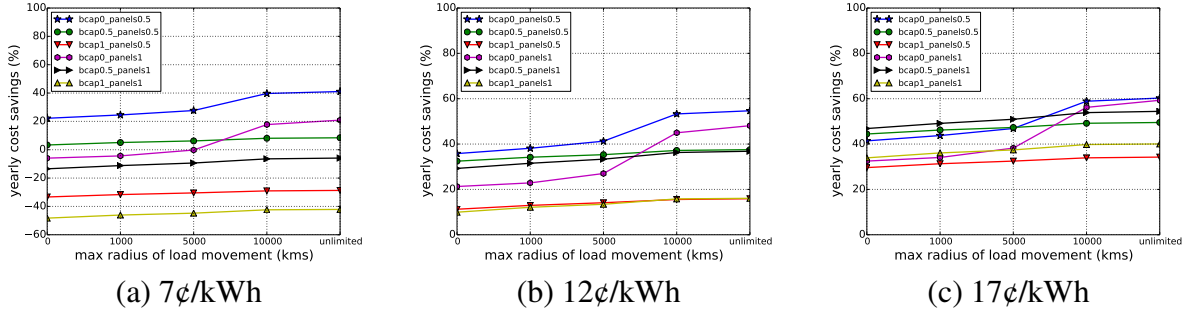


Figure 5.8: Plots show significant amortized savings for moderate and high energy prices. For the lower energy price, we see losses for higher battery capacity and larger number of panels. However, even for the lower energy price, we see significant savings without batteries, and we can see some savings with bcap0.5.

- **Moderate Price - 12¢/kWh:** This is based on a blended value of 12¢/kWh midway between our low and high cost values of 7¢/kWh and 17¢/kWh.
- **High Price -17¢/kWh:** This is on the higher end of the non-household energy prices found in countries in Europe [26].

5.5.4.1 Yearly Amortized Cost Savings

We calculate *original yearly cost* of brown energy drawn from the grid for the original trace. We then calculate the *new yearly cost* of brown energy for the new reduced load after incorporating solar panels, OAC and load movement (for $r > 0$) under the greedy heuristic algorithm. To account for the yearly cost of panels and batteries, we calculate expense for panels and batteries and amortize the price over their lifetime to determine the *yearly amortized cost* for these investments. We then add the *yearly amortized cost* to the *new yearly cost*. Finally, we find the percentage reduction in cost using the *original yearly cost* and *new yearly cost* calculated above. The results for the metric are discussed below.

- **Cost savings are directly proportional to the price of energy:** From Figure 5.8 we see higher savings in cost as we move from a low to a moderate to a high energy price. With a higher per unit energy price, every unit of brown energy drawn from the grid that is replaced with green energy reduces a larger amount from the operational cost.

- *Significant cost savings for moderate and high energy prices:* As seen in Figure 5.8, significant cost savings can be achieved for moderate and high energy prices (plots b and c). Savings range from 9.9% to 60.3% based on different parameter values. With moderate energy prices, for $bcap_{0.5}$ and $panels_{0.5}$, we can see a savings of about 32% without any load movement. For the higher price and same battery size and panels, savings are much higher at 44.4%.

- *Savings in some cases with low energy prices:* From Figure 5.8 (a), we see that with lower energy prices, we can yield cost savings if we employ fewer number of panels ($0.5n_{zy}$) coupled with either no batteries or batteries with a smaller capacity of $bcap_{0.5}$. With $panels_{0.5}$ and $bcap_0$, we see savings ranging from 22% to 41% depending on r . With $panels_{0.5}$ and $bcap_{0.5}$, we see a savings of 3% to about 8.4% depending on r . For other combinations of panels and battery capacities, we incur a loss. However, with prices of solar panel installation and batteries on the decline, we expect these cost savings in this case to improve going forward.

- *Middle ground provisioning:* As seen from the green line in subplots of Figure 5.8, $bcap_{0.5}$ and $panels_{0.5}$ yields no losses for the low energy price and yields significant savings for the higher energy price. This coupled with the fact that $bcap_{0.5}$ and $panels_{0.5}$ yields significant average percent brown energy reduction, (73% for 0.5 net-zero year panels and over 89% with net-zero year number of panels), makes it a good middle ground for achieving both objectives of reducing brown energy consumption and saving on cost.

- *Sensitivity of metric in inversely proportional to energy price:* Generally speaking, this metric is more sensitive to change in parameters (i.e. battery capacity and number of panels) with lower energy prices, as compared to higher energy prices. Observing Figure 5.8, we see that the lines successively span out less as we go from low to moderate to high prices. For the lower energy price for $r=0$, the savings range from 22% to -48%. For the moderate energy price, savings range from about 35.8% to about 10%. Finally, for the higher energy price, savings range from 46% to about 29%. Therefore, decisions to switch between

different battery capacities and number of panels have a greater effect on cost savings when prices are low, as compared to when they are higher.

5.5.4.2 Break-even Analysis

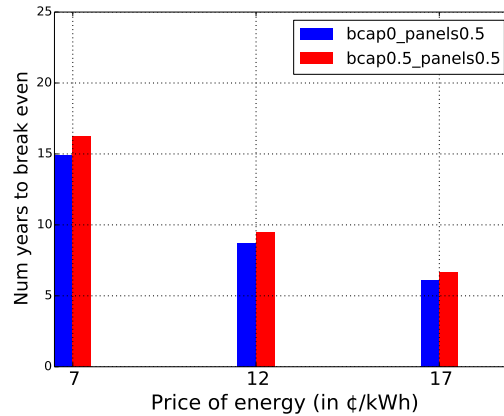


Figure 5.9: Plot shows a decrease in the number of years to break even as the price of energy goes up (for $r=0$).

In this section, we look at the number of years it takes to break even on the expenditure made towards batteries and solar panels. We determine brown energy cost for the year for the original trace and for the new trace after our algorithm has been run. We calculate the difference of these two to get cost savings for the year. We then find the capital expenditure incurred on batteries and solar panels across the IDS, and divide it by the savings for the year to get the number of years it would take to recover the cost.

Figure 5.10 gives an idea of the break-even period across different combinations of battery capacity and panels. Figure 5.9 focuses on $r=0$ and the combination of panels and battery capacity for which the number of break-even years are the lowest:

- *Break-even period is inversely proportional to energy price:* Figure 5.9 shows that for half the nzy panels and a low energy price, we see a break-even period of about 14.9 years. This falls to 8.7 years for the moderate price, and 6 years for the higher price of energy. The same trend is observed for all combinations of panels and capacities as seen in Figure 5.10. Therefore, the higher the price of energy, the lower the number of years to break even. This

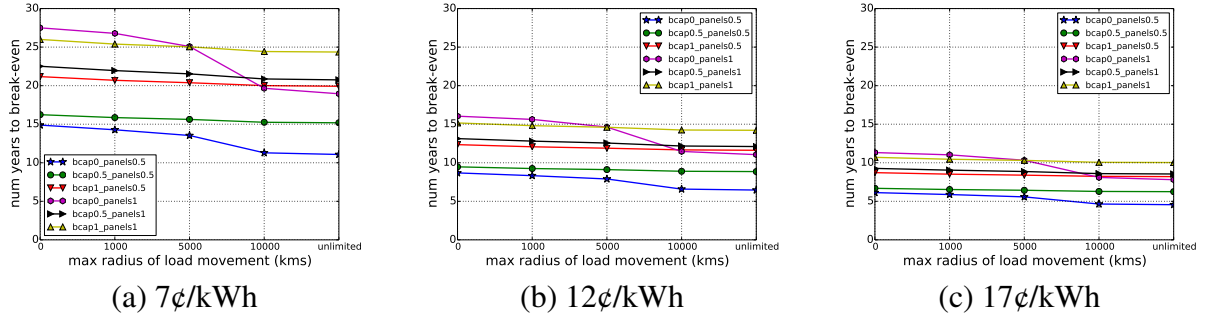


Figure 5.10: The break even period is inversely proportional to the price of energy. With a moderate amount of battery capacity and panels, we can achieve close to the lowest break even periods compared to others.

is because for every unit of brown energy reduced, we get larger savings when we multiply it with the higher unit cost of energy versus a lower unit cost of energy.

- *Finding a middle ground:* The break-even period is very similar for 1) bcap0 and panels0.5; and 2) bcap0.5 and panels0.5. For the higher energy price and with bcap0 and panels0.5, it takes between about 4.6 to 6.1 years to break even depending upon the values of r . With bcap0.5 and panels0.5, it takes about the same number of years (between 6.7 to 6.3) to break-even. This trend is also observed for lower and moderate energy prices as well. Therefore, from a overall solution standpoint considering bcap0.5 is useful in brown energy reduction and cost savings, bcap0.5 and panels0.5 emerges as the preferred option between 1 and 2.

5.5.5 Cost Analysis with Future Projections

Given the price of solar panels and batteries is on the decline, and the price of energy is on the rise, we evaluated our algorithm for 2030 price projections of electricity, solar panels, and batteries. For electricity prices, we used the projected average US electricity price in 2030 [59], we then calculated the current ratio of the average price across all sectors to the current industrial price of electricity [7] to determine the industrial electricity price for 2030. We then used the percentage increase in price to scale up our low, moderate and high prices used in the paper. We used the SunShot study targets for installed solar panel cost in \$/Watt

Parameter	Cost (constant 2017 dollars)
Lower Electricity Cost Projection (¢/kWh)	7.98
Moderate Electricity Cost Projection (¢/kWh)	13.67
Higher Electricity Cost Projection (¢/kWh)	19.36
Solar Panel Cost (\$/Wac)	1.30
Battery Cost (\$/kWh)	70

Table 5.4: Projected Electricity, Solar Panel and Battery Costs

in the beyond 2020 [71] as well as their 2030 targets [64], in conjunction with the current commercial solar panel per watt rates [51] to determine the installed cost of commercial panels in 2030. We used the Bloomberg New Energy Finance (BNEF) projection for the lithium-ion battery cost in 2030 [14]. Table 5.4 shows the projected values we used (in constant 2017 dollars). As a simplifying assumption we assumed that the lifetime of batteries and solar panels remains the same as the current values uses. If the lifetime were to increase in the future, that would yield even higher cost savings.

With the projected values of parameters discussed above, we re-looked at how well the algorithm performs with respect to: 1) yearly amortized cost savings for our algorithm and 2) break-even analysis. Our findings are discussed below:

5.5.5.1 Yearly Amortized Cost Savings with Future Cost Projections

As seen in Figure 5.11, cost savings showed a dramatic increase across the board for all combinations of parameters. Figure 5.11 (a) shows that for the lower price of energy, range from 23.9% to 55.9%. None of the combinations of parameters result in a loss, like we saw with current prices. From Figure 5.11 (b) shows that with moderate energy prices, we can see savings of 38.6% to 68.9%. With the future higher energy price, we see even higher savings ranging from 44.7% to 77.06%.

5.5.5.2 Break-even Analysis with Future Cost Projections

We see a huge decrease in the number of years it takes to break even with the projected prices. From Figures 5.9 and 5.12, we can see that for $bcap_0$, $panels_{0.5}$ and $r=0$, for the

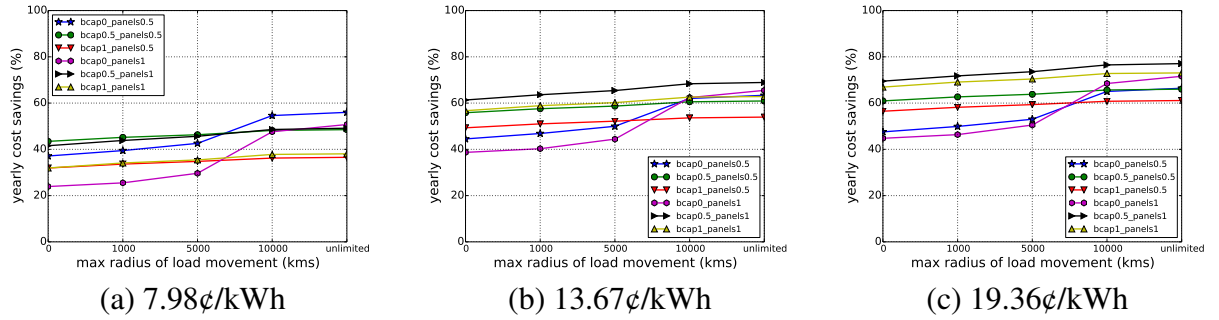


Figure 5.11: Future projection plots show dramatic increases in amortized savings for moderate and high energy prices. For the lower energy price scenario for $r=0$, we see a savings of 23.9% to 55.9% with no losses for any combination. This is an improvement from the current price scenario.

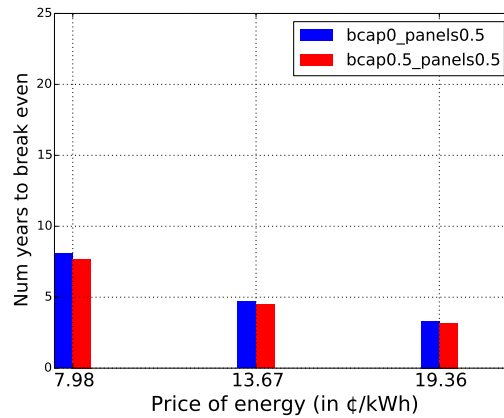


Figure 5.12: Plot shows a significant decrease in the number of years to break-even with future cost projections (for $r=0$).

new low price, the number of years it takes to break even falls from 14.9 years to 8.08 years. For the moderate price it falls from 8.7 to 4.71, and from 6.1 to 3.33 for the high price. We see the similar trend for bcap0.5, panels0.5 and $r=0$ where the number of years are reduced by approximately half between the current and projected costs. In addition, we see from Figure 5.12, that the break even years with bcap0.5 are marginally less than without batteries. Given the decrease in the prices of batteries and solar panels, and the higher energy cost, for 0.5nzy panels in the future it would in fact take marginally less time break even if we employ a battery capacity of bcap0.5, than if we do not have any batteries at all.

5.5.6 Discussion

Our analysis shows that combining solar energy and OAC can significantly reduce brown energy consumption in IDSs. Load movement and batteries can yield further savings. We find that savings due to load movement are most pronounced over larger distances where the night-day difference is apparent. Therefore applications that are not latency sensitive have the most to gain from load movement. Batteries with a capacity of half of the average day's load can significantly increase savings. We also see that batteries not only increase savings, but are also cost effective with moderate and high energy prices. Therefore in locations where energy prices are moderate to high, deploying batteries with solar panels is beneficial. With lower energy prices we can achieve cost savings in certain cases. With future projected prices of solar panels, batteries and energy, we find dramatic increases in cost savings and break even periods for all prices.

5.6 Related Work

Given energy efficiency is important for sustainability, significant work has been done in the area of data centers energy management. Part of this work has focused on reducing energy at the server level. Work includes shutting off servers during off-peak times and switching between high and low power states to prevent wear and tear [60] [44] [49] [17]. Allocation of energy between user applications taking into account user priorities and the lifetime of the battery has also been studied [72]. Prior work has also looked at OS level power management by real-time monitoring of the CPU to keep it utilized to a certain percentage [55].

Separately, another part of prior work has focused on energy-efficiency at the data center level. Job scheduling to maximize solar energy usage without violating user deadlines has been studied [29] [30]. Prior work has looked at using solar energy and wind energy prediction to increase green energy usage and cut down canceled jobs [9]. There has been work on job migration between two sets of servers (one powered by energy from the grid

and another by wind energy) with the goal of maximizing wind energy usage [41]. Prior work has also looked at energy capacity planning finding the best ratio of renewables given a location and workload or given carbon footprint goals [15] [58]. Given cooling accounts for a large portion of data center energy consumption, work has also been done on use of cooling technologies in modular data centers [38] and on unified management of data centers depending upon renewable availability, cooling efficiency, workload fluctuations, and price of energy [16]. Although the above work provides excellent solutions for data center energy management, it is not targeted towards a network-level setting, which is the focus of this paper.

There has been significant prior on network-level energy management as well. Studies have investigated the use of load balancing using the ‘follow the renewables’ approach to almost entirely power their data centers using a renewable mix of wind and solar energy [46] [47]. Prior work has also studied user request routing for greening data centers [66]. Solutions have been proposed for dispatching requests to data centers in a way that maximizes renewable energy and stays within a budget [73]. Work has been done to assign users to data centers based on the three-way mix of latency, price of electricity, and carbon footprint [27]. Prior work has also looked into site selection for green data centers using a follow-the-renewables approach [13]. However, none of these studies explicitly consider a combination of solar energy and open air cooling as part of their renewable mix. Most of them do not evaluate their solution on as extensive real-world, global trace as we have done in our paper. These studies also do not explicitly consider the impact of varying storage capacities on their outcomes. Efficient provisioning of solar panels for net-zero IDSs based on geographical solar energy availability has been previously studied [34]. However, this work is for offline panel provisioning, In contrast, we do not focus on solar panel provisioning, and instead we assume that solar panels are installed at every data center location. Existing work has also looked at geographical load movement to study the potential of open air cooling for serving the cooling energy needs of IDSs [33]. However,

in this paper, we study the *combined* potential of solar energy and OAC for net-zero IDSs, considering both *server energy* and *cooling energy* while determining data center energy demand.

5.7 Conclusions

In this paper, we studied the greening potential of solar energy in conjunction with OAC given their contrasting natures. To that end, we implemented a simple greedy heuristic and evaluated it on an extensive Akamai load trace. We considered several metrics broadly analyzing brown energy reduction and cost effectiveness of employing a combination of solar energy and OAC in IDSs. We found that just by introducing OAC alone to the mix of 0.5nzy panels, brown energy reduction increases from 34% to about 54.9%. With nzy panels, we can go from 41.5% to about 59.4% savings. We can increase our savings further to between 60% to 65% by adding load movement within a radius of 5000kms. With batteries and $r=0$, we are able to significantly reduce brown energy consumption by 73% (for 0.5nzy panels) and over 89% (for nzy panels). We could also achieve peak energy reduction of about 10% to 40%. Therefore the combination of solar energy and OAC enables significant brown energy savings. Our cost analysis showed that for moderate to higher prices of energy we can achieve significant cost savings from 9.9% to 60.3%. For low energy prices, we found that we can still achieve between 22% to 41% savings with panels0.5 and bcap0. For bcap0.5 panels0.5, we see small savings of between 3% to 8.4%. In other cases with a low energy price, we incurred a loss. With a higher price of energy, we could observe break-even periods as low as 6 to 8.7 years. With energy prices on the rise and solar and battery prices declining, we re-looked at the potential under projected prices. We saw dramatic increases in cost savings, with savings between 23.9% to 55.9% even for the lower projected energy price. With $r=0$ and panels0.5, the number of break-even years reduced significantly by roughly 45% for bcap0 and by roughly 50% for bcap0.5. Overall, we showed that the combination of solar energy and OAC has significant greening potential for IDSs.

CHAPTER 6

CONCLUSIONS AND FUTURE WORK

6.1 Conclusions

This thesis has explored greening of IDSs using OAC and solar energy. We first studied the optimal solar provisioning of solar panels for net-zero IDSs. We developed and studied heuristic and optimal algorithms that can help minimize the number of panels provisioned by taking advantage of solar output in global locations. Using our heuristic and optimal algorithms, we are able to significantly reduce the number of solar panels needed for serving load in our datacenters. Given the reduction we see in the number of panels, our findings are significant for including solar into the design of IDSs.

We then focused on OAC to reduce the energy usage as well as the operational and capital costs incurred by an IDS for cooling its servers. We developed algorithms to leverage OAC and to incorporate it into the IDS architecture. We empirically evaluated its efficacy using extensive traces from Akamai’s global CDN and global weather data from NOAA. We showed that OAC can help significantly reduce cooling costs, even in the summer months. In addition, given ASHRAE’s new and less constrained temperature requirements, in some cases, we can virtually eliminate cooling costs for IDSs. These findings coupled with the fact cooling energy requirements are almost as high as server energy requirements, have significant implications for future IDS growth and sustainability.

Finally, we studied the greening potential of solar energy in conjunction with OAC given their contrasting natures. To that end, we implemented a simple greedy heuristic and evaluated it on an extensive Akamai load trace. We considered several metrics broadly analyzing brown energy reduction and cost effectiveness of employing a combination of

solar energy and OAC in IDSs. Overall, we showed that the combination of solar energy and OAC has significant greening potential for IDSs.

6.2 Lessons Learned

Our results and analysis have the following implications:

- Provisioning panels at locations with high solar output coupled with load movement helps in dramatically reducing the number of panels we need to be net-zero. The number of panels varies inversely with the size of the net-zero time window. Out of net-zero year, month and week, the smallest number of panels needed are for the net-zero year scenario. Considering a year is often the industry standard time period over which buildings must be net-zero [36], the implications for low number of solar panels for net-zero year is encouraging. To the extent possible, IDSs should provision more panels at locations with high solar output and employ load shifting to reduce the number of solar panels needed to be net-zero.
- Our OAC study shows that IDSs with A1 data centers can benefit significantly by moving load to leverage OAC. Although we move load to leverage OAC, we found latency does not increase by a large amount for IDS users. With ASHRAE's more relaxed limits on temperature and humidity for A2 through A4 data centers, IDSs can now take advantage of OAC even when operating in hot and humid climates. Therefore, IDSs should be designed to incorporate OAC based load shifting and significantly reduce the expense of cooling their data centers.
- Combining solar energy and OAC leads to a significant reduction in brown energy consumption. Batteries and load shifting help significantly. As a middle ground value, using a battery capacity of half an average day's load, and half the number of panels one needs to be net-zero year yields significant brown energy reduction of about 73% and is cost effective even with low prices of electricity. There are multiple ways (or

combinations of parameters) to achieve a similar gain in brown energy reduction. E.g. $bcap=0$, $panels=0.5$, $r=10,000$ yields similar savings to $panels=0.5$ $bcap=0.5$ with $r=0$. The former can be used for latency-tolerant applications, and the latter can be employed for more latency-sensitive applications though with an added battery cost. Therefore, with the suggested solution it is possible to customize parameters values based on the needs of the application. With the price of renewables and batteries projected to decrease, and the prices of electricity projected to increase in the future, the proposed solution to combine solar energy and OAC will become even more attractive. Overall, IDNs will benefit from using solar energy and OAC in conjunction with each other, employing batteries and load shifting based on the needs of the applications.

As such, any internet-scale distributed system that is characterized by a global deployment of servers and replication of services can benefit from the solutions suggested in this thesis. IDSs that offer latency-tolerant applications e.g. software downloads, security patches, on-demand video will benefit from combining solar energy and OAC facilitated by net-metering, storage and load shifting. However, though IDSs that have latency-sensitive applications like interactive applications, HD video streaming, online gaming, interacting with banks in real time, online trading might not be able to tolerate load shifting over large r , they will still benefit from combining solar energy, OAC, along with net-metering and storage.

6.3 Future Work

There are many avenues for future work some of which we discuss below.

6.3.1 Exploring wind energy

In this thesis, we focused on two sources of renewable energy, namely solar energy and OAC. As part of future work, I would like to explore how our results change if one of both of these renewable sources are replaced with wind energy. Wind energy generation is not

dependent on sunlight and can therefore be available during night-time as well. However, wind turbines require significant upfront capital investment and real estate for installation. As a result, wind turbines are not suitable for urban locations where real estate is at a premium. Therefore, it would be beneficial to quantify gains from using different sources of renewable energy in the same setting so a comparison can be made regarding their viability.

6.3.2 Data center site selection based on renewable energy availability

In the current setting for this thesis, data center locations were fixed. I would like to study if we can improve our results if we have the ability to pick data center locations based on the availability of renewable energy derived from a combination of sources.

BIBLIOGRAPHY

- [1] *Apple Data Centers*. https://images.apple.com/environment/pdf/Apple_Environmental_Responsibility_Report_2017.pdf.
- [2] *Energy Sage Solar Output Temperature*. <http://news.energysage.com/solar-panel-temperature-overheating/>.
- [3] *Fixed or Tracking Array*. <https://pveducation.com/solar-concepts/fixed-or-tracking-array/>.
- [4] *Google Data Centers*. <https://www.google.com/about/datacenters/renewable/>.
- [5] *Net Metering*. <http://www.seia.org/policy/distributed-solar/net-metering>.
- [6] *PV Education Tilt Angles*. <http://www.pveducation.org/pvcdrom/properties-sunlight/solar-radiation-tilted-surface>.
- [7] Administration, U.S. Energy Information. *Industrial Price of Energy US*, 2018. <http://bit.ly/2QnN6vv>.
- [8] Akoush, S., Sohan, R., Rice, A., Moore, A. W., and Hopper, A. Free lunch: Exploiting renewable energy for computing. In *Proceedings of the 13th USENIX Conference on Hot Topics in Operating Systems* (2011), pp. 17–17.
- [9] Aksanli, B., Venkatesh, J., Zhang, L., and Rosing, T. Utilizing green energy prediction to schedule mixed batch and service jobs in data centers. In *Proceedings of the 4th Workshop on Power-Aware Computing and Systems* (2011), pp. 5:1–5:5.
- [10] *Apple To Build Solar Farm To Power Data Center*. <http://www.computerworld.com/article/3161732/sustainable-it/apple-to-build-200mw-solar-farm-to-power-data-center.html>.
- [11] Arlitt, M., Bash, C., Blagodurov, S., Chen, Y., Christian, T., Gmach, D., Hyser, C., Kumari, N., Liu, Z., Marwah, M., McReynolds, A., Patel, C., Shah, A., Wang, Z., and Zhou, R. Towards the design and operation of net-zero energy data centers. In *13th InterSociety Conference on Thermal and Thermomechanical Phenomena in Electronic Systems* (2012), pp. 552–561.
- [12] Barroso, L., and Holzle, U. The case for energy-proportional computing. *IEEE Computer* (2007), 33–37.
- [13] Berral, J. L., Goiri, Í, Nguyen, T. D., Gavaldà, R., Torres, J., and Bianchini, R. Building green cloud services at low cost. In *IEEE 34th International Conference on Distributed Computing Systems* (2014), pp. 449–460.

- [14] *BNEF New Energy Outlook 2018*, 2018. <https://bit.ly/20r3NDE>.
- [15] Brown, M., and Renau, J. Rerack: Power simulation for data centers with renewable energy generation. *SIGMETRICS Perform. Eval. Rev.* 39, 3 (2011), 77–81.
- [16] Chen, T., Wang, X., and Giannakis, G. B. Cooling-aware energy and workload management in data centers via stochastic optimization. *IEEE Journal of Selected Topics in Signal Processing* 10, 2 (2016), 402–415.
- [17] Chen, Y., Das, A., Qin, W., Sivasubramaniam, A., Wang, Q., and Gautam, N. Managing server energy and operational costs in hosting centers. In *Proceedings of the 2005 ACM SIGMETRICS International Conference on Measurement and Modeling of Computer Systems* (2005), pp. 303–314.
- [18] Cormen, T. H., Leiserson, C. E., Rivest, R. L., and Stein, C. *Introduction to Algorithms*, third ed. The MIT Press, 2009.
- [19] *DC Cooling Systems*. http://www.apc.com/salestools/VAVR-5UDTU5/VAVR-5UDTU5_R2_EN.pdf?sdirect=true.
- [20] Dobos, A. P. *PVWatts Version 5 Manual*, 2014. <http://www.nrel.gov/docs/fy14osti/62641.pdf>.
- [21] El-Sayed., N., Stefanovici, I., Amvrosiadis., G., Hwang, A., and Schroeder, B. Temperature management in data centers: Why some (might) like it hot. In *Proceedings of ACM Sigmetrics* (2012), pp. 163–174.
- [22] Endo, H., Kodama, H., Fukuda, H., Sugimoto, T., Horie, T., and Kondo, M. Effect of climatic conditions on energy consumption in direct fresh-air container data centers. In *Proc. of IEEE Intl. Green Computing Conference* (2013), pp. 1–10.
- [23] *How Long Will My Solar Panels Last?*, 2018. <https://bit.ly/2Khnr3k>.
- [24] *Evaluating Solar Panel Efficiency*, 2019. <https://www.energysage.com/solar/buyers-guide/solar-panel-efficiency/>.
- [25] *Solar Panel Power Rating*. <https://www.energysage.com/solar/buyers-guide/solar-panel-efficiency/>.
- [26] *Non-household Price of Energy Germany*, 2018. https://ec.europa.eu/eurostat/statistics-explained/index.php/Electricity_price_statistics.
- [27] Gao, P. X., Curtis, A. R., Wong, B., and Keshav, S. It’s not easy being green. *SIGCOMM Comput. Commun. Rev.* 42, 4 (2012), 211–222.
- [28] Goiri, Í, Katsak, W., Le, K., Nguyen, T. D., and Bianchini, R. Parasol and greenswitch: Managing datacenters powered by renewable energy. *SIGARCH Comput. Archit. News* 41, 1 (2013), 51–64.
- [29] Goiri, Í, Le, K., Haque, Md. E., Beauchea, R., Nguyen, T. D., Guitart, J., Torres, J., and Bianchini, R. Greenslot: Scheduling energy consumption in green datacenters. In *Proceedings of 2011 International Conference for High Performance Computing, Networking, Storage and Analysis* (2011), pp. 20:1–20:11.

- [30] Goiri, Í, Le, K., Nguyen, T. D., Guitart, J., Torres, J., and Bianchini, R. Greenhadoop: Leveraging green energy in data-processing frameworks. In *Proceedings of the 7th ACM European Conference on Computer Systems* (2012), pp. 57–70.
- [31] Goiri, Í., Nguyen, T., and Bianchini, R. Coolair: Temperature-and variation-aware management for free-cooled datacenters. In *Proceedings of the Twentieth International Conference on Architectural Support for Programming Languages and Operating Systems* (2015), pp. 253–265.
- [32] Google To Power Dutch Data Center With Solar Energy. <http://www.businessinsider.com/r-google-to-power-dutch-data-center-with-solar-energy-2017-7>.
- [33] Gupta, V., Lee, S., Shenoy, P., Sitaraman, R. K., and Urgaonkar, R. How to cool internet-scale distributed networks on the cheap. In *Proceedings of the Seventh International Conference on Future Energy Systems* (2016), pp. 9:1–9:12.
- [34] Gupta, V., Shenoy, P., and Sitaraman, R. K. Efficient solar provisioning for net-zero internet-scale distributed networks. In *2018 10th International Conference on Communication Systems Networks* (2018), pp. 372–379.
- [35] Harvey, T., Patterson, M., and Bean, J. Updated air-side free cooling maps: The impact of ASHRAE 2011 allowable ranges. *The Green Grid* (2012). <https://bit.ly/2TM7WFs>.
- [36] K. Peterson, P. Torcellini, R. Grant. A Common Definition for Zero Energy Buildings. <http://bit.ly/2Wr6hL8>.
- [37] Kaune, S., Pussep., K., Leng, C., Kovacevic, A., Tyson, G., and Steinmetz, R. Modelling the internet delay space based on geographical locations. In *Parallel, Distributed and Network-based Processing, 2009 17th Euromicro International Conference on* (2009), pp. 301–310.
- [38] Khalid, R., Wemhoff, A. P., and Joshi, Y. Energy and exergy analysis of modular data centers. *IEEE Transactions on Components, Packaging and Manufacturing Technology PP*, 99 (2017), 1–13.
- [39] Krioukov, A., Alspaugh, S., Mohan, P., Dawson-Haggerty, S., Culler, D. E., and Katz, R. H. Design and evaluation of an energy agile computing cluster. Tech. Rep. UCB/EECS-2012-13, EECS Department, University of California, Berkeley, 2012.
- [40] Li, C., Hu, Y., Gu, J., Jingling, Y., and Li, T. Oasis: Scaling out datacenter sustainably and economically. *IEEE Transactions on Parallel and Distributed Systems* 28, 7 (2017), 1960–1973.
- [41] Li, C., Qouneh, A., and Li, T. iswitch: Coordinating and optimizing renewable energy powered server clusters. In *2012 39th Annual International Symposium on Computer Architecture (ISCA)* (2012), pp. 512–523.
- [42] Li, C., Zhang, W., Cho, C., and Li, T. Solarcore: Solar energy driven multi-core architecture power management. In *Proceedings of the 2011 IEEE 17th International Symposium on High Performance Computer Architecture* (2011), pp. 205–216.

- [43] Lin, M., Wierman, A., Andrew, L., and Thereska, E. Dynamic right-sizing for power-proportional data centers. In *Proc. IEEE INFOCOM* (2011), pp. 1098–1106.
- [44] Lin, M., Wierman, A., Andrew, L., and Thereska, E. Dynamic right-sizing for power-proportional data centers. *IEEE/ACM Trans. Netw.* 21, 5 (2013), 1378–1391.
- [45] Liu, Z., Chen, Y., Bash, C., Wierman, A., Gmach, D., Wang, Z., Marwah, M., and Hyser, C. Renewable and cooling aware workload management for sustainable data centers. In *Proceedings of ACM Sigmetrics* (2012), pp. 175–186.
- [46] Liu, Z., Lin, M., Wierman, A., Low, S. H., and Andrew, L. Geographical load balancing with renewables. *SIGMETRICS Performance Evaluation Review* 39, 3 (2011), 62–66.
- [47] Liu, Z., Lin, M., Wierman, A., Low, S. H., and Andrew, L. Greening geographical load balancing. In *Proceedings of the ACM SIGMETRICS Joint International Conference on Measurement and Modeling of Computer Systems* (2011), pp. 233–244.
- [48] Manousakis, I., Goiri, Í., Sankar, S., Nguyen, T., and Ricardo, B. Coolprovision: Underprovisioning datacenter cooling. In *ACM Symposium on Cloud Computing* (2015), pp. 356–367.
- [49] Mathew, V., Sitaraman, R. K., and Shenoy, P. Energy-efficient content delivery networks using cluster shutdown. In *International Green Computing Conference* (2013), pp. 1–10.
- [50] NOAA Ranking of Cities Based on Percentage Possible Sunshine, 2004. <https://bit.ly/2S9aalD>.
- [51] U.S. Solar Photovoltaic System Cost Benchmark: Q1 2018, 2018. <https://www.nrel.gov/docs/fy19osti/72399.pdf>.
- [52] PVWatts V5, 2014. <https://developer.nrel.gov/docs/solar/pvwatts-v5/>.
- [53] Nygren, E., Sitaraman, R. K., and Sun, J. The Akamai Network: A Platform for High-Performance Internet Applications. *ACM SIGOPS Operating Systems Review* 44, 3 (2010), 2–19.
- [54] ASHRAE Guidelines Enable Year Round Free Cooling. <http://www.datacenterjournal.com/ashrae-guidelines-enable-year-round-free-cooling/>.
- [55] Pallipadi, V., and Starikovskiy, A. The ondemand governor: Past, present and future. In *Proceedings of Linux Symposium* (2006), pp. 223–238.
- [56] Pelley, S., Meisner, D., Wenisch, T., and VanGilder, J. Understanding and abstracting total data center power. In *Workshop on Energy-Efficient Design* (2009).
- [57] Qureshi, A., Weber, R., Balakrishnan, H., Gutttag, J., and Maggs, B. Cutting the electric bill for internet-scale systems. In *Proceedings of the ACM SIGCOMM 2009 conference on Data communication* (2009), pp. 123–134.
- [58] Ren, C., Wang, D., Urgaonkar, B., and Sivasubramaniam, A. Carbon-aware energy capacity planning for datacenters. In *Proceedings of the 2012 IEEE 20th International Symposium on Modeling, Analysis and Simulation of Computer and Telecommunication Systems* (2012), pp. 391–400.

- [59] Schwartz, L., et al. *Electricity End Uses, Energy Efficiency, and Distributed Energy Resources Baseline*, 2017. <https://bit.ly/2D1Gqci>.
- [60] Sharma, N., Barker, S., Irwin, D., and Shenoy, P. Blink: Managing server clusters on intermittent power. *SIGARCH Comput. Archit. News* 39, 1 (2011), 185–198.
- [61] Shehabi, A., Smith, S. J., Sartor, D. A., Brown, R. E., Herrlin, M., Koomey, J. G., Masanet, E. R., Horner, N., Azevedo, I. L., and Lintner, W. *United States Data Center Energy Usage Report*. http://eta-publications.lbl.gov/sites/default/files/lbnl-1005775_v2.pdf.
- [62] Sheme, E., Frashëri, N., Holmbacka, S., Lafond, S., and Luzanin, D. Datacenters powered by renewable energy: A case study for 60 degrees latitude north. In *24th International Conference on Software, Telecommunications and Computer Networks* (2016), p. 1–5.
- [63] Smith, K., Saxon, A., Keyser, M., Lundstrom, B., Cao, Ziwei, and Roc, A. Life prediction model for grid-connected li-ion battery energy storage system. In *2017 American Control Conference* (2017), pp. 4062–4068.
- [64] *The SunShot 2030 Goals*, 2017. <https://bit.ly/2AUqexf>.
- [65] *Solar Energy SEIA*. <http://www.seia.org/about/solar-energy>.
- [66] Stewart, C., and Shen, K. Some joules are more precious than others: Managing renewable energy in the datacenter. In *SOSP Workshop on Power Aware Computing and Systems* (2009).
- [67] *Climate and Weather Averages in Anchorage*, 2019. <https://bit.ly/2HImswT>.
- [68] Treacy, M. Facebook Uses Open-Air Cooling in Super Efficient N.C. Data Center. <http://goo.gl/ZM1FdJ>.
- [69] *The Average PUE is 1.8: Uptime Institute*. <http://bit.ly/1eEqN9d>.
- [70] Weerts, B., Gallaher, D., Weaver, R., and Geet, O. Van. Green data center cooling: Achieving 90% reduction: Airside economization and unique indirect evaporative cooling. In *Proc. of IEEE Green Technologies Conference* (2012), pp. 1–6.
- [71] Woodhouse, M., et al. *The Role of Advancements in Solar Photovoltaic Efficiency, Reliability, and Costs*, 2016. <https://www.nrel.gov/docs/fy16osti/65872.pdf>.
- [72] Zeng, H., Ellis, C. S., Lebeck, A. R., and Vahdat, A. Ecosystem: Managing energy as a first class operating system resource. *SIGPLAN Not.* 37, 10 (2002), 123–132.
- [73] Zhang, Y., Wang, Y., and Wang, X. Greenware: Greening cloud-scale data centers to maximize the use of renewable energy. In *Middleware* (2011), vol. 7049, pp. 143–164.